Review

Molecular Imaging of Inflammation in Atherosclerosis

Moritz Wildgruber[1✉], Filip K. Swirski[2], Alma Zernecke[3,4✉]

1. Department of Radiology, Klinikum Rechts der Isar, Technische Universität München, Germany;
2. Center for Systems Biology, Massachusetts General Hospital, Harvard Medical School, Boston, USA;
3. Department of Vascular Surgery, Klinikum Rechts der Isar, Technische Universität München, Germany;
4. Deutsches Zentrum für Herz-Kreislauf Forschung (German Research Center for Cardiovascular Research), partner site Munich Heart Alliance, Munich, Germany.

✉ Corresponding author: Moritz Wildgruber MD, PhD or Alma Zernecke MD. Department of Radiology, Klinikum Rechts der Isar, Technische Universität München, Ismaninger Strasse 22, D-81675 München, Germany. Phone: +49-89-4140-2621 Fax: +49-89-4140-4834 email: moritz.wildgruber@tum.de or zernecke@lrz.tum.de.

Abstract

Acute rupture of vulnerable plaques frequently leads to myocardial infarction and stroke. Within the last decades, several cellular and molecular players have been identified that promote atherosclerotic lesion formation, maturation and plaque rupture. It is now widely recognized that inflammation of the vessel wall and distinct leukocyte subsets are involved throughout all phases of atherosclerotic lesion development. The mechanisms that render a stable plaque unstable and prone to rupture, however, remain unknown and the identification of the vulnerable plaque remains a major challenge in cardiovascular medicine. Imaging technologies used in the clinic offer minimal information about the underlying biology and potential risk for rupture. New imaging technologies are therefore being developed, and in the preclinical setting have enabled new and dynamic insights into the vessel wall for a better understanding of this complex disease. Molecular imaging has the potential to track biological processes, such as the activity of cellular and molecular biomarkers *in vivo* and over time. Similarly, novel imaging technologies specifically detect effects of therapies that aim to stabilize vulnerable plaques and silence vascular inflammation. Here we will review the potential of established and new molecular imaging technologies in the setting of atherosclerosis, and discuss the cumbersome steps required for translating molecular imaging approaches into the clinic.

Key words: Molecular imaging, Inflammation, Atherosclerosis

Inflammation in Atherosclerosis

Atherosclerotic cardiovascular disease is an increasingly common disease and contributes considerably to mortality and morbidity worldwide. Atherogenesis is driven by a combination of disturbed equilibrium of lipid accumulation and maladaptive immune responses. The disease entails chronic inflammation of the arterial wall and cross-talk with procoagulant pathways, culminating in plaque rupture and atherothrombosis. Atherosclerosis is characterized by arterial lesions that progress from an initial fatty streak towards an unstable (vulnerable) plaque in the arterial vessel wall. Early atherosclerotic lesion development is triggered by endothelial dysfunction and the local deposition of lipids (e.g. low density lipoprotein), particularly at sites of hemodynamic strain. In the intima, lipoproteins are prone to oxidative modifications and subsequently activate endothelial cells and intimal resident or infiltrated immune cells, causing a local inflammatory response that sustains leukocyte recruitment to the vessel wall. Monocytes that ingest excess lipids differentiate into macrophages and foam cells. The more advanced stable plaque consists of a thick fibrous cap with high collagen and smooth muscle cell content and a lipid core containing foam cells, debris and lipid droplets. The presence of an intact advanced plaque may lead to a

stenotic obstruction of the blood vessel (e.g. the coronary artery), a phenomenon which may clinically manifest as angina pectoris. Mechanisms that still largely remain unknown can render a stable plaque unstable and prone to rupture. Plaque rupture results in exposure of the plaque's prothrombotic core contents and leads to massive local blood coagulation and formation of a thrombus. Such thrombosis may lead to local and/or distal obstruction of blood vessels and gives rise to the major part of acute myocardial infarctions and stroke. Notably, plaque rupture is the most common type of plaque complication, accounting for ≈70% of fatal acute myocardial infarctions and/or sudden coronary deaths [1-4].

While animal models of disease have greatly advanced our understanding of the molecular mechanisms and cellular players underlying atherogenesis, atheroprogression and atherothrombosis as the pathogenetic sequence of CAD, the greatest challenge in cardiovascular medicine remains the identification of unstable or vulnerable (but often non-obstructive) arterial plaques that may be prone rupture. Although sensitivity, specificity, and overall predictive value of potential factors remain to be conclusively defined, criteria have been defined that make a plaque more likely to rupture. These include active inflammation, often defined as extensive macrophage accumulations, a thin fibrous cap with a large lipid core, superficial erosion and platelet aggregation or fibrin deposition, a fissured plaque cap and severe stenosis [1].

The development and refinement of non-invasive imaging therefore aims at providing reliable tools for the identification of preclinical disease and unstable lesions that reach beyond identification of flow-limiting stenosis. We here review molecular imaging modalities and discuss the cellular and molecular targets for imaging in the clinic.

Modalities for non-invasive Molecular Imaging

Imaging has become an indispensable tool both in cardiovascular research and clinical care within the last decades. Various imaging technologies are now available that each have their strengths and weaknesses (Table 1). Imaging in the clinical theatre is mostly restricted to depicting anatomy and quantifying the degree of vessel stenosis. However, more and more approaches aiming at the detection and characterization of vulnerable plaques are being translated into patient care [5, 6]. Molecular imaging of atherosclerosis is challenging as the vessels move rapidly with heart beat and respiration and most vessels of interest are in close proximity to tissue interfaces such as lung, blood or myocardium which can cause disturbing artifacts or strong background signal. ECG

and respiratory triggering have facilitated data acquisition and lead to a significant improvement in image quality. When evaluating and comparing modalities for Molecular imaging both spatial resolution and temporal resolution are considered key properties of an imaging system. Spatial resolution describes a systems's ability to separate two closely spaced objects, or with respect to molecular imaging two closely spaced molecular probe concentrations. The higher the spatial resolution is, the higher the possibility to detect subtle molecular signals emitted from a cell or a molecular probe. Similarly, temporal resolution describes the ability to discriminate between two points in time. The temporal resolution is especially important when dynamic imaging is performed to track the kinetics of probe accumulation over time as well as when CINE imaging of moving/pulsating structures is performed. Sometimes there is a tradeoff between temporal and spatial resolution, and the temporal resolution theoretically achievable by a certain modality may be hampered by the special resolution and vice versa.

Nuclear Imaging Techniques and Computed Tomography

As nuclear imaging approaches are covered elsewhere in this issue only few important points relevant to multimodality approaches shall be mentioned here.

The most important disadvantage of both PET and SPECT is their limited spatial resolution. Small animal PET can resolve structures at ~1-2mm resolution, whereas clinical PET is limited to 4-5mm maximum spatial resolution. Such physical limitations make it unlikely that PET's spatial resolution will improve significantly[5], however the limited spatial resolution may be compensated by hybrid imaging. PET-CT combines the excellent spatial resolution of CT with the high sensitivity in probe detection of the PET. A relevant concern using PET-CT is the radiation dose of ~10mSv a patient is exposed during imaging[7]. While CT offers only limited capabilities to differentiate various plaque components, recent integration of PET and MRI promises a significant advance for non-invasive characterization of vulnerable plaques. Combination of PET with MRI instead of CT significantly reduces radiation exposure due to replacement of the x-ray radiation, which is especially important for whole-body imaging. In comparison, average radiation exposure of coronary artery catheterization is ~7mSv, a SPECT based sestamibi stress test ~9mSv and coronary CT ~4-15mSv (depending on the technique used and the patient's size). When comparing nuclear imaging techniques, cost and availability have to be taken into account. Short-lived

PET tracers require a cyclotron facility nearby the imaging site, while longer-lived SPECT tracers can be provided from outside sources. The minor costs of SPECT compared to PET have led to a broad availability in clinical medicine.

CT is able to detect and accurately quantify vessel calcification, and coronary calcium scoring has been used as a risk predictor for future cardiovascular events. However, three-quarters of all coronary lesions are non-calcified plaques and high-risk vulnerable plaques prone to rupture usually do not contain significant calcifications [8-11]. With the help of iodinated contrast agents such non-calcified plaques can be detected. Improvements in multislice detector technology now enable the visualization of coronary anatomy in addition to large vessels with rapid (seconds) acquisition and minimal motion artifact. Similarly, novel reconstruction algorithms enable a significant dose reduction, making coronary CT attractive for wide applications. Moreover, detection of plaque inflammation using CT has been achieved by using N1177, an iodine containing agent taken up by macrophages [12]. Gold nanorods may become an attractive alternative as they are able to yield good contrast on CT imaging and can be coupled to gadolinium (Gd) compounds, NIR fluorochromes and nuclear tracers for multimodal imaging and be additionally used as drug carriers for various theranostic applications [13-15].

Table 1: Non-invasive Modalities for Molecular Imaging of Atherosclerosis

Technique	Spacial Resolution	Depth	Acquisition Time	Quantitative	Imaging Agents	Molecular Targets	Clinical application	Specific Features
MRI	10-100μm	No limit	min-h	Yes	Gd-Chelates, superparamagnetic nanoparticles (SPIO, USPIO, VSOP)	Adhesion Molecules, Macrophages, pro-inflammatory enzymes (myeloperoxidase), Lipoproteins, Apoptosis/Necrosis, Integrins, Fibrin	Quantification of stenosis, Plaque morphology, Flow measurements	+ No radiation + high-soft-tissue contrast
CT	50μm	No limit	sec-min	Yes	Iodinated molecules	Calcification	Plaque morphology, Coronary Plaque burden	- Radiation - high spatial and temporal resolution
Ultrasound	50μm	cm	sec-min	Yes	Microbubbles	Adhesion molecules, Integrins, Glycoproteins	Plaque Morphology, Intima-Media Thickness, Flow velocities	- Operator-dependent + high temporal resolution
PET	~ 2mm	No limit	min-h	Yes*	^{18}F, ^{64}Cu, ^{11}C Tracers	FDG, Adhesion Molecules, Integrins, Fibrin, Ca^{2+}hydroxyapatite	Plaque inflammation	- Radiation - Cyclotron required - limited spatial resolution - stand alone PET not quantitative (overcome by hybrid PET/CT)
SPECT	~ 2mm	No limit	min-h	Yes	^{99m}Tc, $^{123/124/125/131}$I, ^{111}In Tracers	Adhesion moleculaes, Lipoproteins, Macrophages, Proteases, Glycoproteins, Apoptosis	Myocardial Perfusion Imaging	- Radiation - limited spatial resolution -full quantification only by hybrid SPECT/CT -lower costs and higher availability compared to PET
Bioluminescence Imaging	2-5mm	Few cm	min	No	Luciferins	Gene expression, Cell tracking	No	- Experimental only - limited spatial resolution
Fluorescence Molecular Tomography	1mm	Few cm	min	Yes*	NIR fluorochromes	Adhesion molecules, Monocyte/Macrophages, Proteases, Collagen, Ca^{2+}hydroxyapatite, Thrombosis	Not yet	-semiquantitative only (improved by hybrid FMT/CT) - experimental only (Clinical applications under development)
Optoacoustic Imaging	<50μm	Few cm	min-h	Yes	NIR Fluorochromes	targets comparable to FMT	Catheter applications (see Table 2)	-Interference with hemoglobin -experimental only

(+) advantage, (-) disadvantage
*when hybridized with CT/MRI for proper attenuation correction

Magnetic Resonance Imaging

MRI provides high spatial and temporal resolution and has the advantage of combining anatomic, functional and molecular imaging in an all-in-one approach. Its high soft tissue contrast enables to distinguish the major components of atherosclerotic plaques and allows risk stratifications based on plaque composition irrespective of the degree of stenosis [16, 17]. Contrast enhanced MRI enables highly sensitive molecular imaging of vulnerable plaques. Paramagnetic gadolinium based agents provide enhance contrast by shortening the spin-lattice relaxation time (T1). Superparamagnetic iron-oxide nanoparticles, which target the phagocytic capacity of plaque-infiltrating leukocytes, consist of an iron-oxide core and a surrounding shell made of dextran, synthetic polymers or polyvinyl alcohol. Depending on their size these nanoparticles are classified as SPIO (small superparamagnetic iron oxide, >60nm), USPIO (ultra-small superparamagnetic iron oxide, <60nm) and VSOP (very small superparamagnetic iron oxide, <10nm) particles. The size of the particles affects their extravasation and biodistribution, as well as the mode of elimination from the body. Upon contact, these particles are rapidly taken up by phagocytic cells *in vitro* and *in vivo*. Superparamagnetic iron-oxide particles influence signal intensity mainly by shortening T2* and T2, which at a given echo time produces darkening of the contrast-enhanced tissue. Conversely, they can act as positive agents (T1 shortening and image brightening) when appropriate imaging sequences are used [18]. The USPIO/SPIO derived MRI signal correlates highly with macrophage presence in murine, rabbit and human atheroma [19-23]. The dextran or alcohol shell of the nanoparticles can be used to conjugate antibodies or other peptides for targeted imaging. In contrast, conjugation of high-affinity ligands to Gd-based paramagnetic agents is more difficult. A new and elegant tool for targeting mononuclear phagocytes is to pack micelles or liposomes with Gd agents, thereby reducing toxicity [24, 25]. A more sophisticated approach is the synthesis of activatable MR contrast agents that lead to signal amplification upon specific binding[26, 27].

Ultrasound

Molecular imaging using ultrasound-targeted microbubbles to enhance ultrasound contrast may potentially be translated to imaging in patients [28]. A significant obstacle is the strong background signal that decreases detection sensitivity especially in deep vessels such as the coronaries. Yet, targeted microbubbles may not only be used for specific molecular imaging of inflammation and the detection of adhesion molecules, selectins or von-Willebrand Factor [29-32], they can additionally be used as drug carriers for theranostic applications[33]. A detailed overview of molecular imaging of cardiovascular disorders with ultrasound is provided in reference [34].

Fluorescence imaging

Fluorescence techniques have significantly enhanced our understanding of cardiovascular disease. Their high sensitivity, cost-effectiveness and the large portfolio of targeted agents have led to wide applications in preclinical research investigating pathophysiology at the microscopic, mesoscopic and macroscopic scale [26, 27, 35-39]. Fluorescence Molecular Tomography (FMT) technology permits a highly sensitive 3-D detection of enzyme activities [39-41], tissue calcification[42, 43] and integrin expression[44]. The use of fluorescent probes emitting light in the near-infrared (NIR) spectrum allows the detection of molecular signals in living animals in depths of several centimeters [39, 45]. Also, imaging in the NIR region minimizes tissue autofluorescence, thereby improving target to noise ratio.

Near-infrared fluorescence (NIRF) sensors can be constructed in three different ways: 1) Non-specific fluorescent blood-pool agents injected in the circulation of the animal that inform on perfusion or permeability of the tissue, 2) targeted probes that bind via specific ligands to protein structures on the cell surface or 3) 'smart probes', that are activated *in situ* by enzymatic conversion or enzymatic cleavage [35, 46]. These probes have been used to detect enzyme activity in live mice by FMT and with cellular resolution by fluorescence microscopy [43, 47, 48]. Currently, FMT allows the non-invasive detection of fluorochrome concentrations in the pico-molar range in deep tissues with a submilimeter resolution *in vivo*.

Clinical translation of optical imaging is limited by the restricted tissue penetration of NIR light. While non-invasive imaging may be applicable to superficial carotid arteries, deeper vessels would require more invasive assessment. Recent advances in miniaturization of fluorescence light source and detector technology have led to first catheter-based applications.

One challenge of Fluorescence Imaging is the proper signal quantification. As the fluorescent light emitted from the molecular target experiences diffuse scattering and attenuation on its way through complex tissues, full signal quantification is obtained by methods of attenuation correction using similarly acquired CT data [49]. These additional CT data sets can be obtained sequentially after FMT by using multimodal animal holders with fiducial markers [41]. However, the first prototypes of full hybrid FMT-XCT (Fluorescence Molecular Tomography- X-ray Computed Tomography) systems have shown improved

performance by using a dual prior inversion method [50-52].

One advantage of fluorescence molecular imaging is the possibility to subsequently perform traditional *ex vivo* laboratory techniques. After *in vivo* fluorescence imaging the animal can be sacrificed and the biodistribution of the molecular sensor can be detected and quantified by cryoslicing[53]. Similarly, fluorescence microscopy can be performed on tissue sections after *in vivo* biodistribution of the injected probe; the sections can then be further evaluated *ex vivo* with classical tools such as immunofluorescence, immunohistochemistry, and in situ hybridization. Multicolor flow cytometry is an elegant tool to determine the cellular source of a fluorescence imaging signal obtained non-invasively *in vivo* [40, 47].

Photoacoustic imaging

Photoacoustic imaging is based on the photoacoustic effect, where ultra-short pulses of light that are absorbed in tissue create broadband ultrasound waves, which can be detected non-invasively outside the body. Because ultrasound scatters orders of magnitude less compared to fluorescence light in tissue it can provide optical images with a spatial resolution of ~50μm. By using multiple excitation wavelengths and tomographic signal detection, Multispectral Optoacoustic Imaging (MSOT) can provide images of specific chromophores including organic dyes as well as nanoparticles based on their unique spectra[37, 54]. First preclinical applications of MSOT in cardiovascular research have achieved successful anatomic visualization of the heart and major blood vessels as well as high-resolution imaging of inflammation in a model of acute myocardial infarction. First *ex vivo* studies with specimens from patients with symptomatic carotid artery disease have demonstrated that MSOT is capable of rendering detailed biodistribution of MMP activity together with high-resolution images of vulnerable plaques [55].

Intravascular Molecular Imaging

Intravascular catheter-based imaging techniques have contributed significantly to the understanding of human atherosclerosis. An overview of the specific features of existing techniques and their advantages or disadvantages is provided in Table 2. Intravascular Ultrasound (IVUS) is able to provide high-resolution images of the vessel wall and plaque morphology at an axial resolution of ~100μm using high-frequency detectors (up to 45 MHz). Spectral analysis of the IVUS backscatter radiofrequency signal enables color-coded images of certain plaque characteristics, referred to as virtual histology (IVUS-VH) [56]. With high spatial resolution this technique is able to differentiate lipid-rich areas, the necrotic core, fibrous tissue and calcifications on the basis of different echolucent structures [57]. With increased spatial resolution of 10-15μm optical coherence tomography (OCT) has facilitated the characterization of neointimal hyperplasia following percutaneous coronary intervention (PCI), and has allowed for depiction of the internal and external elastic lamina as well as a thin fibrous cap (<65μm)[58-60]. The drawback of OCT is the inability to image in the blood stream because the small wave lengths reflect very small objects such as blood cells. Further improvement of conventional time-domain OCT has been achieved by introducing frequency domain OCT (also referred to as OFDI, Optical frequency Domain Imaging), where a Fourier transformation of the acquired spectra enables to image at much higher frame rates of >100 frames/s. This allows fast 3D image acquisition of long vessel segments under a single non-occlusive saline flush without occluding the vessel [61].

Intravascular radiation detector systems have been tested for endovascular sensing of ^{18}F-FDG in atherosclerotic lesions. Various systems were able to detect ^{18}F point sources in the canine femoral as well as in the coronary arteries using an open chest model [62]. Using a model of femoral artery denudation in hypercholesterolemic rabbit's intravascular ^{18}F detection in injured artery segments correlated with increased macrophage content [63]. Miniaturized catheters systems were even able to detect increased ^{18}F accumulation in murine aortas of apoE$^{-/-}$ mice [64]. The catheter based ^{18}F detection may be superior to regular PET/SPECT as spatial mapping of the probe distribution within the lesion may be improved.

Intravascular NIRF Imaging is an attractive approach for human coronary artery imaging and has the potential to identify vulnerable plaques upon the high macrophage load as well as increased protease activity. A first study in hypercholesterolemic rabbits has demonstrated that this technique can detect the fluorescent signal emitted from a previously injected protease sensor activated in plaques within the iliac artery [65]. Further improvement of the technique has led to engineering of new catheter capable of 2D fluorescence imaging in a 360° view during automated pullback. This improvement enabled a submilimeter axial resolution, nanomolar sensitivity to the injected NIR probe and only moderate light attenuation by the circulating blood [66]. The whole system was based on a 2.9F angiography catheter and thus potentially applicable to human coronary arteries. In a recent report intravascular NIRF imaging has been combined with OFDI technology for molecular and microstructural imaging of atherosclerosis [67]. Intravascular MSOT approaches similarly aim to provide

high-resolution anatomical images of the atherosclerotic plaque and to report on the biological activity by using targeted molecular probes [68]. The successful preclinical application of these intravascular molecular imaging approaches in various animal models will pave the route for first human trials with the aim to detect vulnerable plaques prior to percutaneous coronary intervention via a transarterial approach.

Table 2: Invasive Modalities for Molecular Imaging of Atherosclerosis

Technique	Spacial Resolution	Depth	Acquisition Time	Quanti-tative	Imaging Agents	Molecular Targets	Clinical application	Specific Features
OCT	~10 µm	2-3mm	min	Yes	-	-	Plaque and thrombus charcterization	- Blood-free field required
OFDI	~10 µm	2-3mm	min	Yes	-	-	Plaque and thrombus charcterization	+ Faster image acquisition compared to OCT
IVUS-VH	~100µm	10mm	min	Yes	-	-	Plaque characterization	- Interference with blood at frequencies>40MHz
Angioscopy	10-50µm	Surface Imaging	Min	No	-	-	Imaging of plaque surface, thrombus characterization	- Blood-free field required
Intravascular Fluorescence Imaging	1mm	Few cm	min	Yes	NIR Fluoro-chromes	Macro-phages, Proteases, Apoptosis	Not yet	+ Imaging of arterial inflammation
Intravascular Optoacoustic Imaging	<50µm	Few cm	min	Yes	NIR Fluoro-chromes	targets compara-ble to FMT	Lipid detection in athero-sclerotic plaques	- Interference with he-moglobin + high spatial resolution

(+) advantage, (-) disadvantage

OCT=Optical Coherence Tomography, IVUS-VH=Intravascular Ultrasound-Virtual Histology, OFDI=Optical Frequency Domain Imaging

Cellular and Molecular Targets within the inflamed vessel

Initiating steps of inflammation: shear stress and lipid accumulation

A schematic overview of plaque formation and its' consequences are shown in Figure 1. Atherosclerotic lesions develop in particular predisposed regions of the vasculature. While flow with physiological levels of laminar shear stress in straight segments is regarded as atheroprotective, areas experiencing low and especially oscillatory shear stress or turbulent blood flow such as inner curvatures as well as vessel bifurcations are prone to develop atheroma [69]. Oscillatory shear stress in particular leads to increased activation of the endothelium [70], and it is therefore not surprising that these regions are characterized by a higher inflammatory load and an increase of reactive oxygen species, and accumulate lipids within the intima [71-73]. Simulations based on computational mechanics will help to better understand the effects of wall shear stress on the arterial wall and the associated cellular and molecular adaptations to altered mechanical forces. High-resolution MR Imaging can aid in identifying atherosclerosis-prone areas with altered shear stress [74].

Paving the route for immune cell influx: Endothelial activation and permeability

Endothelial activation one of the initiating steps of vessel inflammation and atherosclerotic lesion development. Upon activation endothelial cells express various adhesion molecules triggering leukocyte recruitment across the blood-vessel wall [75]. Selectins (e-selectin, p-selectin and l-selectin), adhesion molecules such as intercellular adhesion molecule (ICAM)-1 and vascular cell adhesion molecule (VCAM)-1, and chemokines control leukocyte rolling, adhesion and migration into the vessel wall. The adhesion molecule is expressed on activated endothelial cells, smooth muscle cells but also macrophages, and recruits leukocytes via binding of the integrin very late antigen (VLA)-4. Thus, imaging approaches targeting VCAM-1 use VLA-4 peptides, anti-VCAM-1 antibodies and peptides of the MHC-I molecule interacting with VCAM-1. These targeting moieties can be conjugated to various nuclear tracers (^{123}I, ^{99m}Tc, ^{18}F) for PET and SPECT imaging, NIR fluorochromes for intravital microscopy and non-invasive tomo-

graphic optical imaging, iron-oxide based nanoparticles (SPIO) for MRI or microbubbles for CEU [76-84]. These agents have been reported to successfully detect vascular inflammation and atherosclerotic lesions and to correlate with intraplaque VCAM-1 mRNA levels. However, VCAM-1-targeted probes do not exclusively detect activated endothelium, as also activated macrophages express VCAM-1 and other integrins [30, 80, 85]. To enhance uptake and probe accumulation, targeting multiple moieties represents an interesting and promising approach. It has been shown that combined VCAM-1 and selectin targeting leads to > 5-fold binding to activated endothelium compared to single-targeted probes[29, 86, 87]. ICAM-1 targeted mircobubbles as well as a liposomal Gd-based MRI agent are similarly able to visualize activated endothelium and inflammatory atherosclerotic lesions *in vivo* [88, 89]. Selectin-target probes have similarly been engineered for targeting inflammation. A dendritic polyglycerol sulfate based fluorescent probe has been applied to target inflammation within the injured myocardium [90]. The inhibitory properties of this agent impair leukocyte recruitment to sites of inflammation, rendering an agent for both imaging and treatment of atherosclerosis [91].
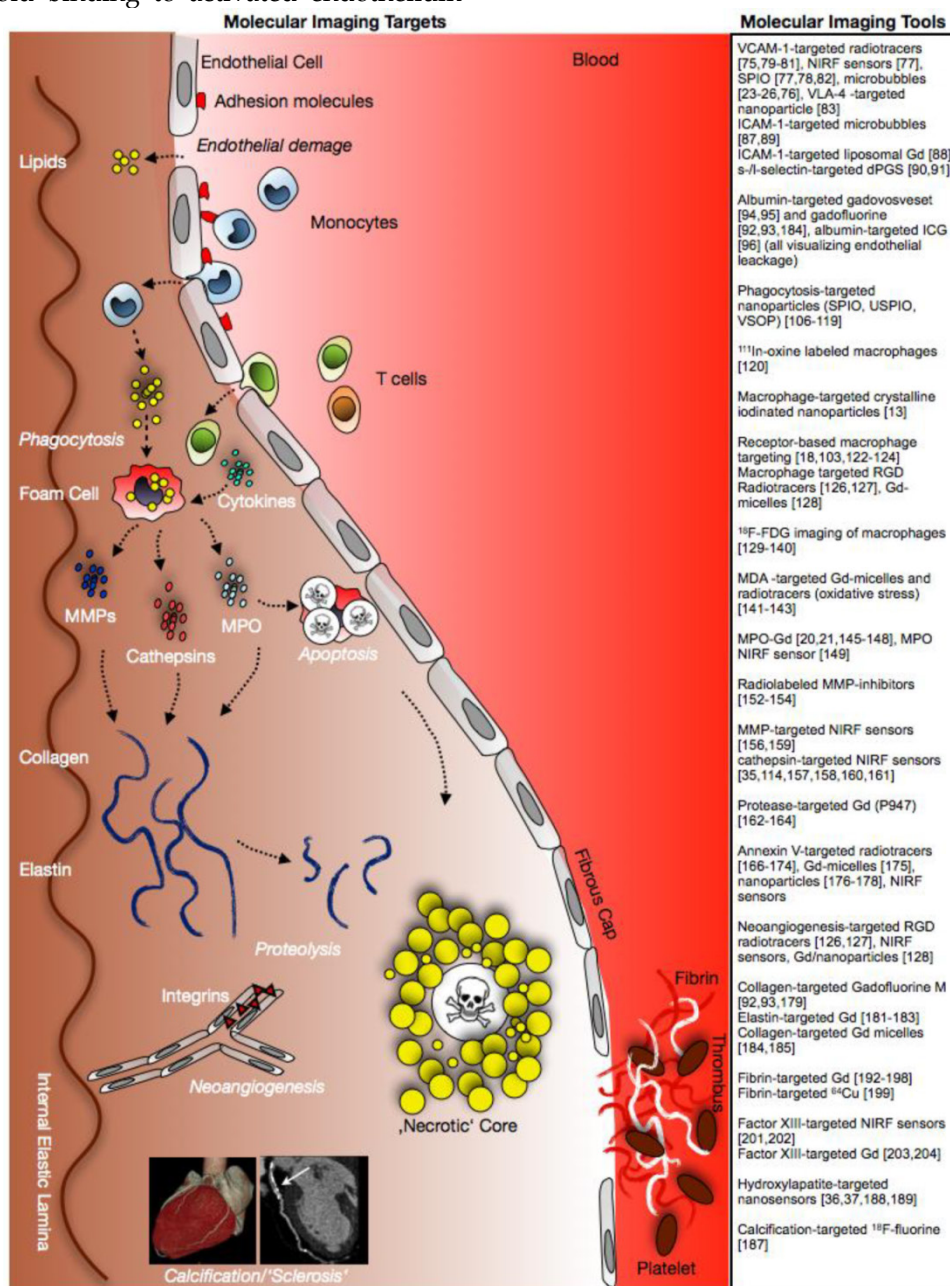

Fig 1. Tools and targets for molecular imaging of atherosclerosis. Figure demonstrates schematic evolution of atherosclerotic plaques and potential targets for molecular imaging.
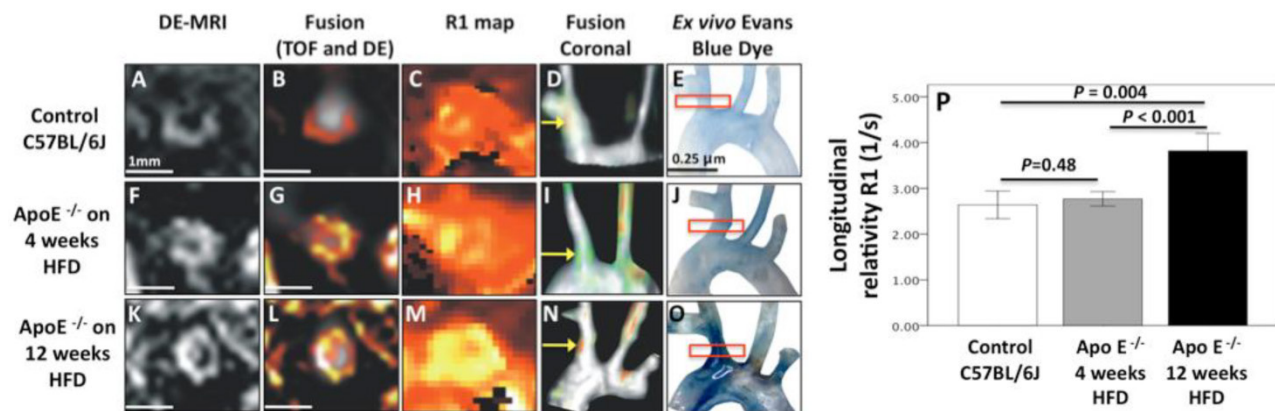
Fig 2. MR Imaging of endothelial permeability. Uptake of gadofosveset in regions of the brachiocephalic artery of control (Panel A-E) and atherosclerotic mice after 4 (Panel F-J) and 12 weeks (Panel K-O) of high-fat diet is associated with endothelial permeability. After 12 weeks significant increase in R1 relaxivity is observed in the inflamed vessel wall following gadofosveset injection (Panel P). Image courtesy of Alkystis Phinikaridou and René M. Botnar, King's College London.

Concomitant to the expression of adhesion molecules, endothelial dysfunction and increased endothelial permeability are considered as initiating events in plaque formation. Progressive endothelial leakage permits low-density lipoproteins to diffuse across the endothelial cell lining and accumulate in the arterial intima. Gadofosveset is a clinically approved albumin-binding contrast agent. Binding of albumin leads to a prolonged half-life within the blood pool and a dramatically higher r1-relaxivity. The uptake of gadofosveset has been linked to mechanically damaged endothelium in a porcine model of coronary injury [92] as well as with atherosclerosis-induced endothelial damage in apoE$^{-/-}$ mice [93]. Figure 2 demonstrates gadofosveset accumulation in atherosclerotic plaques with underlying endothelial damage indicated by a bright contrast in T1-weighted MR images. Similarly, amphiphilic NIR fluorochromes can be used for optical imaging of vulnerable plaques. Indocyanine green (ICG), a clinical approved NIRF dye, also binds to albumin with high affinity and accumulates in atherosclerotic plaques after *in vivo* injection in hypercholesterolemic rabbits as well as after incubation of human carotid artery specimens[94].

Monocyte accumulation, phagocytosis and metabolism

During atherogenesis, monocytes accumulate in the arterial intima and differentiate into macrophages, which then ingest oxidized lipoproteins, secrete a diverse array of proinflammatory mediators, and mature towards foam cells [95, 96]. Monocyte heterogeneity has been conserved in various species [97]. At least two different subpopulations exist with divergent properties. In hypercholesterolemic mice, Ly6C^{hi} (Gr-1$^+$) monocytes preferentially accumulate in lesions [98]. Proinflammatory Ly6C^{hi} monocytes dominate hypercholesterolemia-associated monocytes and give rise to macrophages in atheroma [99]. The role of Ly6C^{lo} monocytes is less clear in atherogenesis, but it appears that these cells exhibit an anti-inflammatory phenotype and play a major role in extracellular matrix formation and tissue remodeling. Also in humans, two major subpopulations have been described. CD14^{lo}CD16^{hi} monocytes (corresponding to Ly6C^{lo} monocytes in mice) display elevated serum levels in patients with coronary artery disease [100, 101] whereas levels of CD14^{hi}CD16^{lo} monocytes (corresponding to Ly6C^{hi} monocytes in mice) are predictive for myocardial salvage after myocardial infarction [102]. Targeting monocytes has been performed using various formulations of superparamagentic nanoparticles.. An example of targeting macrophages in murine atheroma using VSOPs is shown in Figure 3. Interestingly, under anti-inflammatory therapy with atorvastatin leading to a decrease in macrophage activity, uptake of USPIOs was significantly reduced [103]. While murine Ly6C^{hi} and Ly6C^{lo} monocytes exhibit equal phagocytic capacity of cross-linked iron-oxide nanoparticles[104], human CD14^{hi}CD16^{lo} monocytes display a higher phagocytic capacity *in vitro* compared to their CD14^{lo}CD16^{hi} counterparts[101, 105]. This phagocytic phenotype may therefore be well suited for specific targeting of monocyte subsets in patients with atherosclerosis. Imaging of iron-oxide loaded inflammatory macrophages has been successfully performed in animals and humans and constitutes a promising approach for identifying vulnerable plaques[106-108]. While most studies report on the direct injection of the nanoparticles into the circulation, *ex vivo* labeling with subsequent reinjection and recruitment of labeled phagocytes to sites of inflammation has also been utilized [109]. The latter approach may enhance target-to-background signal by eliminating unspecific probe accumulation, yet it has to be considered that *ex*

vivo labeling with iron-oxides affects the phenotype of the labeled cells and potentially their function [105]. *Ex vivo* labeling with ^{111}In-oxine was similarly successful at visualizing macrophage accumulation in murine atherosclerotic lesions [110]. Also nanoparticles can be conjugated to radionuclides as well as NIR fluorescent dyes for hybrid nuclear and optical imaging in conjunction to MRI[47, 81]. Beside targeting the phagocytic capacity of monocytes/macrophages, receptor-based imaging of phagocytes has been reported by using Gd-loaded micelles targeting the macrophage scavenger receptor, the cannabinoid receptor and the neutrophil gelatinase-associated lipocalin 2 (NGAL) in murine plaques[24, 111-113] as well as targeting the MCSF-receptor on human monocyte subsets[101]. Furthermore, activated macrophages in atherosclerotic lesion express various integrins such as $\alpha v \beta 3$. Targeting $\alpha v \beta 3$ using RGD based nuclear tracers[114, 115] as well as MR contrast agents[116] allows identification of activated macrophages in atherosclerotic plaques in various animal models.

Aside from targeting immune cells via their phagocytic capacity or receptor profile, imaging of metabolic activity of the cellular infiltrate has been applied to assess inflammation in atherosclerotic plaques by PET/CT [117-120]. The glucose analogue ^{18}F-FDG is taken up by metabolically active cells, especially by macrophages and foam cells, and thus reports on inflammatory activity in atherosclerotic lesions (Figure 4). First clinical trials of ^{18}F-FDG PET/CT showed strong association between ^{18}F-FDG uptake in carotid artery lesions with type 2 diabetes[121] and more importantly with the occurrence of ischemic stroke[122, 123]. Exciting are the results of the dal-PLAQUE study, one of the first multicenter clinical trials employing non-invasive multimodality imaging, MRI and PET-CT, to assess structural and inflammatory indices as primary endpoints of the effects of dalcetrapib on carotid disease[124]. In patients, the ^{18}F-FDG signal correlates closely with the expression of biomarkers such as GLUT-1, HK2, cathepsin K and CD68 in carotid artery lesions [125]. Interestingly, in a similar approach, the investigators were not able to find significant correlations between ^{18}F-FDG uptake and CD68 levels in patients with peripheral arterial occlusive disease [126]. A recent *ex vivo* study investigated the in vitro uptake of FDG in several cell types involved in atheroma formation, revealing that predominantly hypoxia but not inflammatory cytokines stimulates cells to accumulate FDG,. Therefore FDG uptake signals in atheroma may reflect hypoxia-stimulated macrophages rather than the mere inflammatory burden [127]. Yet these results await further evaluation *in vivo*.

Novel hybrid imaging technologies will be helpful in correlating specific tracer accumulation within the vessel wall/atherosclerotic lesions and lesion morphology when imaged simultaneously by CT or MRI. Figure 5 shows successful ^{18}F-FDG imaging of plaque inflammation in a hypercholesterolemic rabbit by full hybrid MR-PET (Panel A-C) as well as vessel wall inflammation in a patient with large-vessel vasculitis by both PET-CT and MR-PET (Panel D-L). PET-MR may in particular be promising for detection of vulnerable plaques as it combines the molecular information reported by various tracers from the PET with high-resolution and functional imaging by MRI.
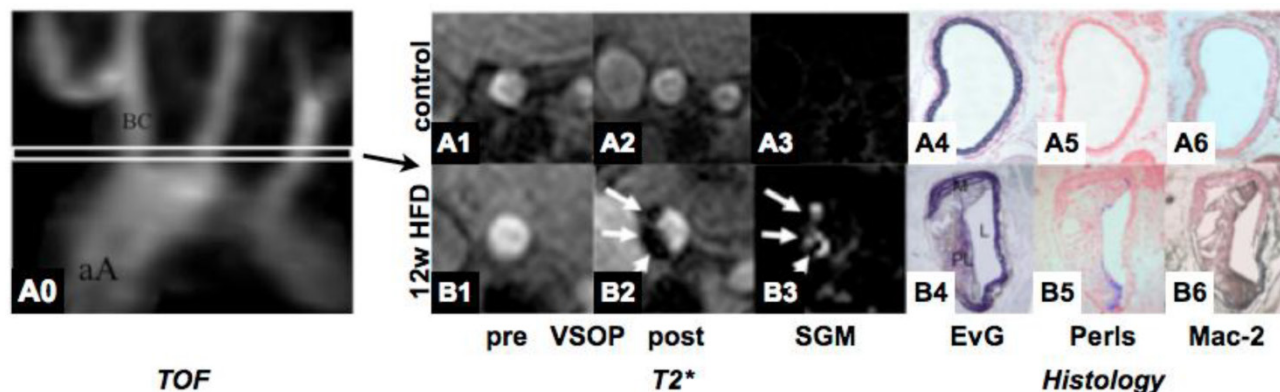

Fig 3. MR Imaging of vascular inflammation using very small superparamagnetic nanoparticles (VSOP). VSOPs target inflammatory macrophages in high-fat diet induced atherosclerosis in mice, inducing shortening of T2* relaxation in the vessel wall in HFD fed mice (lower row) as compared to controls (upper row). Imaging findings are corroborated by histology (A4-A6 and B4-B6). EvG=Elastica van Gieson, HFD=high-fat diet, SGM=susceptibility gradient mapping. TOF=Time-of-Flight angiography. Image courtesy of René M. Botnar, King's College London.
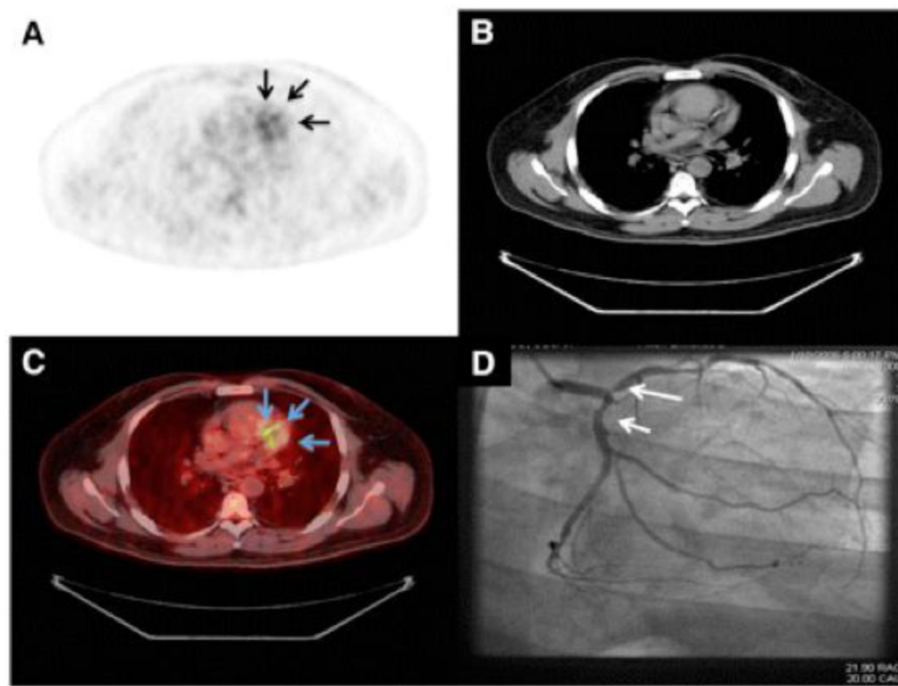
Fig 4. Imaging of the vulnerable plaques in human coronary atherosclerosis. Representative images of ^{18}F-FDG PET (A), CT (B), PET/CT (C), and coronary angiography (D) from patient with good suppression with coronary ^{18}F-FDG uptake (arrows). Reprinted with the permission of the Society of Nuclear Medicine from Wykrzykowska et al. [183]
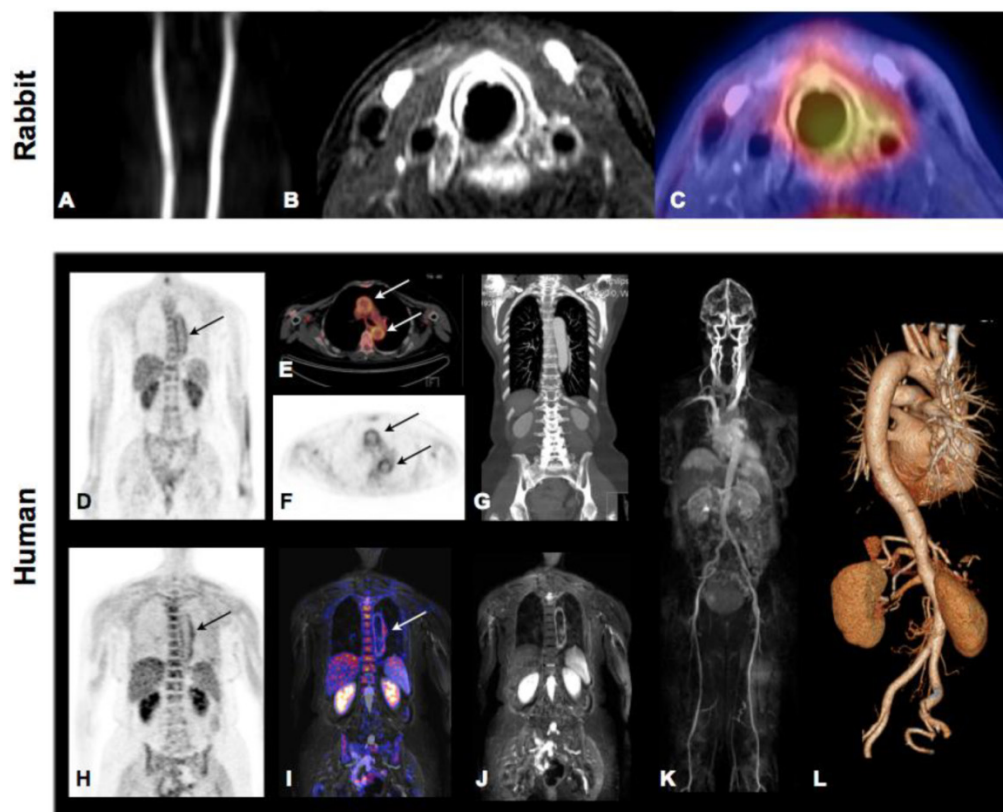

Fig 5. Molecular Imaging of atherosclerosis by hybrid PET-CT and MR-PET. Inflammation in plaques of hypercholesterolemic rabbits can be assessed and quantified by 18F-FDG PET and co-localized to carotid artery by simultaneously acquired MRI. Panel A: TOF angiography, Panel B, contrast enhanced fat-suppressed T1 weighted MRI (delayed enhancement), Panel C: MR-PET fusion showing increase tracer accumulation around the left carotid artery. Images demonstrate good correlation of PET signal and contrast-enhanced MRI but also show limited spatial resolution of PET technology. Hybrid Molecular Imaging in a patient with large-vessel vasculitis (Panels D-L). Increased 18F-FDG uptake can be visualized by whole-body PET and correctly co-localized to the aortic arch by the subsequently performed contrasted enhanced CT (Panels D-G: PET-CT). Similar co-localization can be performed using hybrid MR-PET (Panels H-J). Whole body MRA (Panel K) and CTA (Panel L) can be routinely performed during hybrid image acquisition. Images courtesy of Isabel Dregely, Stefan Nekolla and Ambros J. Beer from the Munich PET/MR consortium of TUM and LMU (funded by DFG).
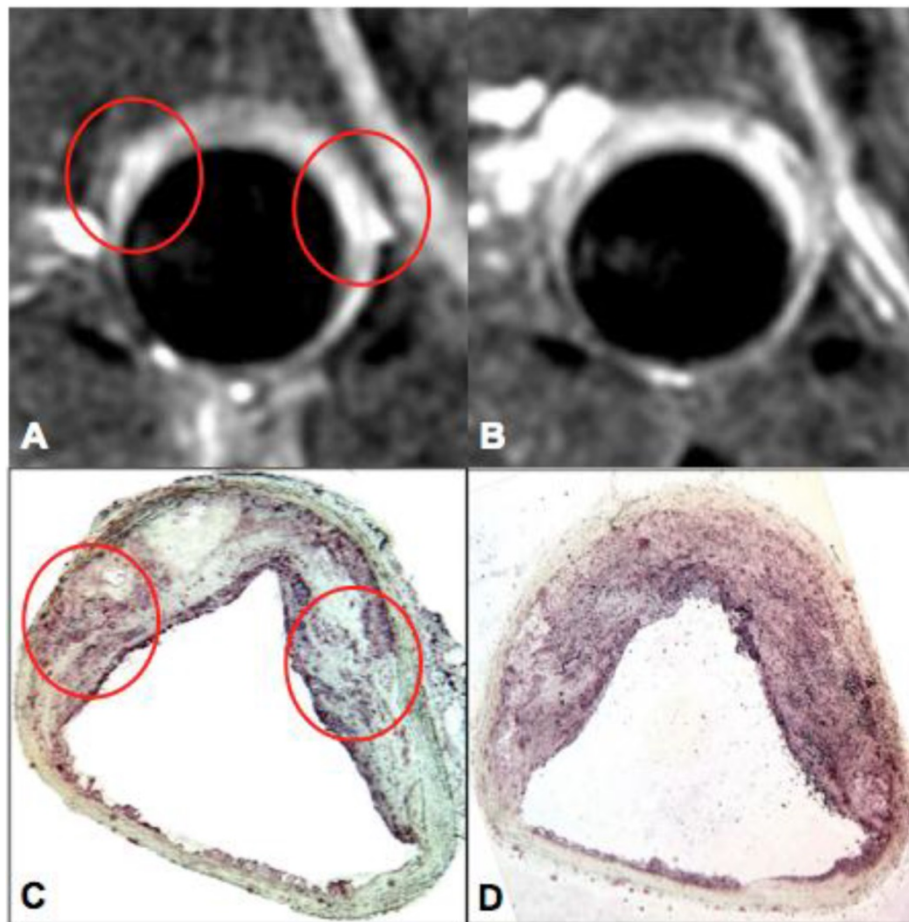
Fig 6. Myeloperoxidase (MPO) – targeted MRI of vascular inflammation. MPO-Gd MR imaging of atherosclerosis in a rabbit model fed high cholesterol diet for 24 months. MPO-Gd imaging identifies areas of high MPO activity and content (red circles) that are corroborated by MPO immunostaining. Images courtesy of John W. Chen, Massachusetts General Hospital, Harvard Medical School.

Lipids and Oxidative Stress

Oxidative stress promotes lipid oxidation and cell death and is one of the major triggers of lesion progression and destabilization. Oxidized lipids have been targeted in preclinical atherosclerosis models using MDA (malondialdehyde-lysine) MR contrast agents [128]. Oxidative stress is predominantly mediated through reactive oxygen species (ROS). In atherosclerotic plaques, ROS are produced by macrophages, neutrophils and smooth muscle cells. A signature enzyme of inflammation and ROS production is myeloperoxidase (MPO). Advanced human atheroma as well as ruptured plaques contains increased numbers of MPO expressing macrophages [129]. Targeting of MPO may therefore be useful for the identification and characterization of vulnerable plaques. A prototype of an amplifiable MRI contrast agent has been reported by Chen et al [26, 27]. This Gd-MPO [bis-5HT-DTPA (Gd)] increases its relaxivity upon contact with MPO; subsequent polymerization and protein binding leads to signal amplification *in situ* compared to its native state. This agent has been applied for molecular imaging of various inflammatory conditions [130, 131] and for targeting inflammation in a rabbit model of atherosclerosis (Figure 6)[132]. Similarly, MPO-sensing in cardiovascular diseases can be achieved by fluorescent nanoparticles detecting hypochlorous acid production *in vivo* [133].

Consequences of infiltrating immune cells: proteolysis and matrix degradation

In concert with the phagocytic activity of other infiltrating immune cells, macrophages in particular secrete proteolytic enzymes which can degrade extracellular matrix proteins promoting thinning and rupture of the fibrous cap [134]. Among the various existing proteases cathepsins and MMPs have most frequently been used for molecular imaging, and targeted by two major strategies. Nuclear tracers based on small molecule protease inhibitors bind to the active site of the enzyme of interest and enrich at sites with a high protease concentration. These MMP inhibitors (MMPI) can be coupled to various radiotracers such as ^{123}I, ^{111}In, ^{99m}Tc or ^{18}F for PET and SPECT imaging. SPECT imaging signal of MMPI has been

shown to correlate to MMP-2/-9 activity in atherosclerotic plaques [135, 136].

Alternatively, optical reporters are being used that are activated upon contact with the target enzyme [137]. The sensor is injected in its inactive state in which fluorochromes are not excitable due to auto-quenching. Proteolytic cleavage of the scaffold releases the fluorochromes and results in extensive fluorescence generation (de-quenching). Amplification is achieved because one active enzyme moiety can activate multiple reporters [39]. Both FMT and Optoacoustic Tomography are able to resolve this process non-invasively in small animals as well as tissue specimens. In a pilot study an activatable NIRF sensor, activated by gelatinases A (MMP2) and B (MMP9), was able to detect MMP activity in aortas of apoE$^{-/-}$ deficient mice on high-cholesterol diet. Both *ex vivo* FRI and *in vivo* FMT yielded high MMP activity compared to injected apoE$^{+/+}$ mice and animals not injected with the probe[138]. Similar to the detection of MMP activity, cathepsin can be detected in inflammatory lesions. Using pan-cathepsin NIRF sensors, high protease activity was detected in atherosclerotic lesions of apoE$^{-/-}$ as well as double knock out apoE$^{-/-}$eNOS$^{-/-}$ mice [139]. Strong co-localization of cathepsin B with macrophages within the lesion pointed towards mononuclear phagocytes as the main source of secreted proteases. Using a combined FMT-CT imaging approach and a variety of nanosensors tracing cathepsin activity, the study localized the molecular fluorescence signal to the aortic root of mutant mice [41]. The combination of FMT and CT further allowed proper quantification of the pan-cathepsin signal and thus allowed to appropriately monitor atorvastatin therapy. The anti-inflammatory effect of statins in atherosclerosis was similarly reported using a cathepsin B-activatable NIRF sensor [140]. While most of the protease sensors discussed report pan-MMP or pan-cathepsin activity, more selective probes become available. A cathepsin K selective optical reporter demonstrated high protease activity by intravital microscopy as well as *ex vivo* FRI [141]. Activity of cathepsin S was associated with vascular calcification and co-localized with an osteogenesis targeted imaging agent in mice with chronic renal disease [142]. With respect to monocyte heterogeneity, as discussed above, these sensors can distinguish increased protease contents in proinflammatory Ly6C^{hi} monocytes as compared to lower activity in Ly6C^{lo} monocyte subsets [104].

The only MRI-based approach targeting proteases has been performed using P947. This gadolinium chelate is coupled to a peptide, which binds MMPs [143, 144]. These pilot results are encouraging; and suggest that a non-invasive imaging approach may be clinically applicable at identifying vulnerable plaques.

The dusk of inflammation: Apoptosis

The three major characteristics of vulnerable plaques are a high degree of inflammation, thinning of the protective fibrous cap and a lipid rich 'necrotic' core. Lipid-laden foam cells are prone to undergo apoptosis [145]. Cell debris further promotes inflammation, secretion of proteases, and thus progressive destabilization of the plaque, ultimately resulting in rupture and thrombosis. During apoptosis, activated flippases rapidly externalize phosphaditylserine (PS) chains from the inner membrane of the lipid double layer to the outer layer of the membrane. The externalized PS are recognized by the 35kD plasma protein Annexin V (A5) [146]. A5 has been used for various molecular imaging approaches both in preclinical atherosclerosis models as well as in human cardiovascular disease. It can be coupled to nuclear tracers, NIRF fluorochromes or iron-oxide nanoparticles for MR imaging. For plaque imaging A5 labeled with ^{99m}Tc proved most suitable both in experimental as well as in first human trials [147]. In atherosclerotic mice, rabbits and swine ^{99m}Tc labeled A5 showed focal tracer accumulation in inflammatory plaques *in vivo*, which correlated with immunohistochemistry of cell death and high macrophage load [148-150]. A pilot report of four patients with symptomatic carotid artery disease revealed high tracer accumulation at the affected carotid bifurcation, and post-endarterectomy histology evaluation confirmed high macrophage load as well as intraplaque hemorrhage [151]. Similarly, SPECT imaging of apoptosis can detect therapeutic effects of anti-inflammatory as well anti-apoptotic regimens in hypercholesterolemic rabbits [152].

An A5 conjugated micellar nanoparticle carrying multiple Gd-labeled lipids for MRI as well as fluorescent lipids for optical imaging was able report on apoptosis and macrophage accumulation in atherosclerotic aortas of apoE$^{-/-}$ mice [153]. Coupling of Annexin V to the dextran shell of superparamagnetic iron-oxide nanoparticles enabled apoptosis imaging by T2* weighted MRI in various models of cardiovascular disease [154, 155].

Yet, PS externalization is not specific to apoptosis but also occurs in activated macrophages and stressed cells in general [146, 149]. This has to be taken into account when evaluating anti-apoptotic therapies by A5-based molecular imaging [152]. Nevertheless, cell stress and macrophage activation are likewise hallmarks of vulnerable plaques, so that cumulative targeting of these aspects of vascular inflammation may in fact enhance probe accumulation and increase contrast in biomedical imaging. Oligo-targeted mo-

lecular imaging that visualizes apoptosis and protease activity may thus enhance *in vivo* imaging signals and study interlinked processes of inflammation in cardiovascular disease [135].

Extracellular Matrix and Vascular Remodeling following active inflammation

During inflammation, increased proteolysis as described above is responsible for the degradation of ECM proteins and subsequent vascular remodeling. Molecular Imaging of ECM proteins has been achieved by MRI using Gadofluorine, a Gd-based contrast agent targeting collagen, proteoglycans and tenascin[156-158]. The ECM protein elastin has been shown to be crucial for arterial remodeling in atherosclerosis. Human atheroma and macrophage-rich plaque regions display a high content of immature disorganized tropoelastin but lack stabilizing cross-linked, mature elastin. Recently an elastin-targeted molecular MR agent (ESMA) has been introduced and showed promising results for non-invasive imaging of the vessel wall (Figure 7). ESMA was able to visualize and quantify plaque burden in atherosclerotic apoE$^{-/-}$ mice [159] and de-

pict stent induced coronary injury in a swine model [160, 161]. Also paramagnetic micelles (CNA35) targeting collagen were able to detect murine atherosclerosis by molecular MRI [162].

The end stage of vascular remodeling is the formation of microcalcifications and sclerosis [163], and there is clear evidence that both inflammation and calcification are closely related to each other[42, 43]. Molecular targeting of vessel wall calcifications has been achieved by fluorescence imaging and hydroxylapatite-targeted PET [42, 43, 164, 165]. Together with high-resolution CT hydroxlyapatite targeted PET may give rise to a more comprehensive evaluation of plaque phenotype, integrating morphology, plaque composition, degree of the resulting vessel obstruction, and stage of plaque progression. Already today, coronary CT is able to distinguish between stable and vulnerable plaques based on the existence and pattern of calcifications. While large calcifications are characteristic of stable plaques, both non-calcified plaques as well as spotty calcifications are more frequently observed in patients presenting with an acute coronary syndrome [166].
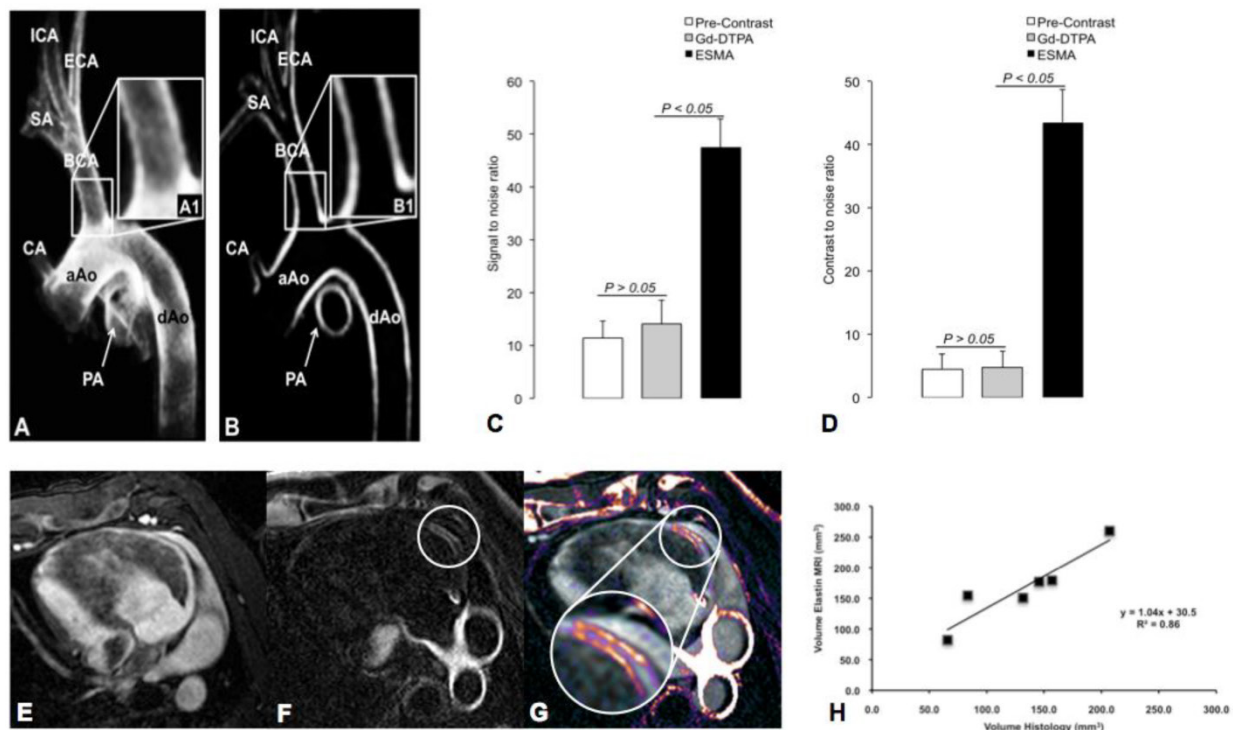

Fig 7. Imaging of Vascular Remodeling. Vascular remodeling can be assessed with an Elastin-targeted Magnetic Resonance Agent (=ESMA). Panels A and B show ESMA-enhanced MR images of the aortic arch and supraaortic vessels in swine wit increased SNR and CNR compared to non-targeted Gd-DTPA (Panel C and D). A similar approach is able to detect vascular injury following coronary stent implantation. Magnetic Resonance Angiography (MRA, Panel E), delayed-enhancement MRI after injection of ESMA (Panel F) and fusion of E and F (Panel G). Quantification of Elastin by MRI yields good correlation with Histology (Panel H). Images courtesy of Marcus Makowski and René M. Botnar, Kings College London and Christian von Bary, Universität Regensburg.

Rupture of the inflamed atherosclerotic plaque and thrombus formation

Rupture of the inflamed atherosclerotic plaque leads to exposure of a variety of prothrombotic plaque constituents to the circulation, initiating athero-thrombosis and sequelae such as the development of stroke or myocardial infarction. Selective targeting of clot-bound platelets has been achieved using peptides or antibodies with high affinity for the glycoprotein IIb/IIIa[167, 168].

Fibrin-targeted MRI has vast potential in thrombus imaging and has already passed Phase I and II clinical studies after promising results in animal models [169-172]. EP-2104R is a Gd-based MR imaging agent functionalized with a short peptide with high affinity to fibrin [173-175]. A novel ^{64}Cu labeled EP-2104R showed promising results in depicting arterial thrombi by hybrid MR-PET in a rat model [176]. Quantification of intraplaque and endothelial fibrin has been achieved by applying novel T1 mapping techniques of the injected EP2104R [177]. An example of this approach is shown in Figure 8.

Another preclinical approach uses peptide substrates for factor XIII, an important factor in cross-linking fibrin monomers for thrombus stabilization. Fluorescent nanosensors were able to reveal factor XIII activity in experimental models of thrombosis and may enable to differentiate acute versus chronic thrombi *in vivo* [178]. Similar approaches using MRI showed feasible factor XIII detection in preclinical animal models [179].
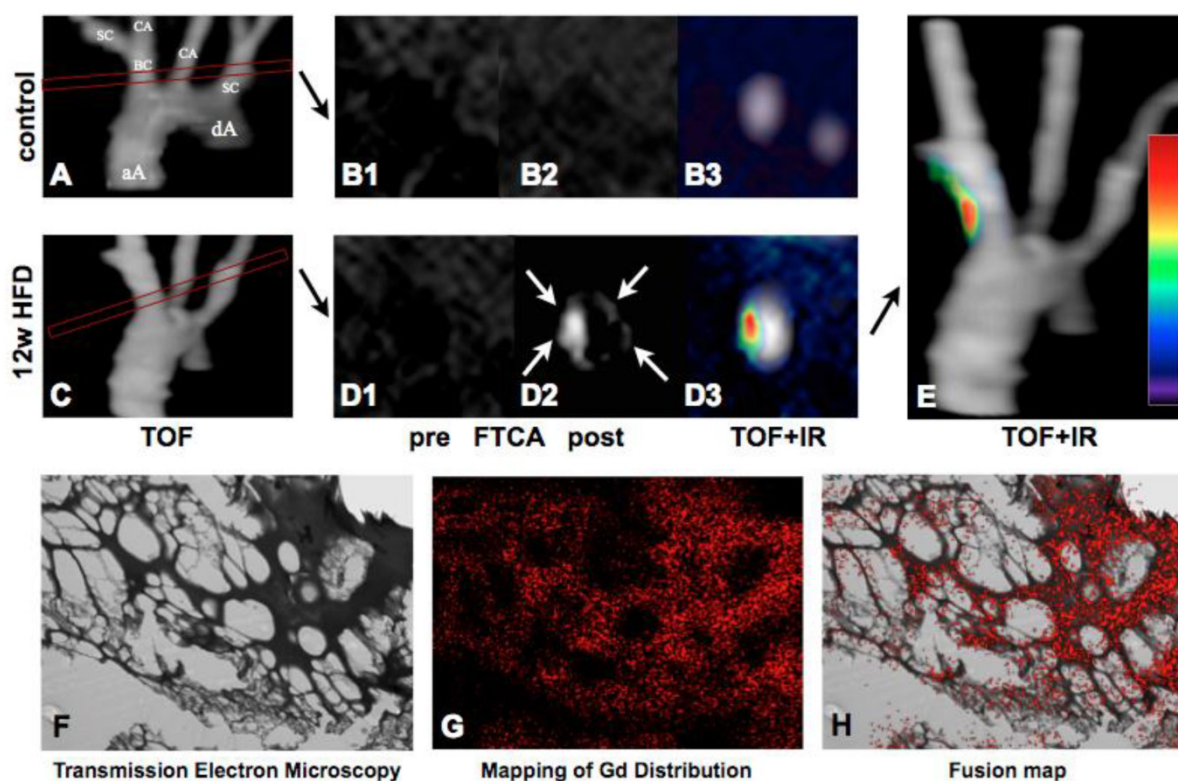

Fig 8. Fibrin-targeted molecular MRI of thrombus formation. 3D TOF images of the aortic arch in a control (Panel A) and ApoE^{-/-} mice (Panel C). The subsequently performed imaging sequences (delayed enhancement and T1 mapping sequences) were aligned perpendicular to the brachiocephalic artery. Atherosclerotic plaques were imaged prior to FTCA in control (B1) and 12 week HFD ApoE^{-/-} mice (D1), and 2 hours after an injection of FTCA (B2-3, D2-3). Delayed enhancement (white arrows) is seen selectively as a white hotspot on the post-contrast images (D2) whilst the signal from the surrounding blood and tissues is suppressed. Fusion of the TOF and late enhancement images confirm signal localization in the vessel wall of the BCA (D3, E). Transmission electron microscopy (F) and mapping of gadolinium distribution (G) in an engineered thrombus. For colocalization experiments thrombus samples were incubated with FTCA. Good colocalization of signal from Gd with the fibrin mesh was found (H). aA: ascending aorta, dA: descending aorta, BC: brachiocephalic artery, IR: inversion recovery, SC: subclavian artery, CA: carotid artery, FTCA: Fibrin targeted contrast agent. Images courtesy of René M. Botnar, King's College London.

Target selection for clinical molecular imaging

As outlined above, a variety of molecular targets have so far been successfully employed in preclinical models of cardiovascular disease. However, the translation of imaging agents and technologies into the clinic has been much slower than anticipated. When selecting potential targets for molecular imaging of patients, the target has to fulfill a set of criteria

to be suitable for non-invasive detection: The expression and kinetics of a potential molecular target should be known in the course of the disease, and the target density at the region of interest should be high enough to be captured with a high contrast-to-noise ratio. Above all, an imaging agent has to be available that is able to detect the target with high sensitivity and specificity, is non-toxic, and preferably available at low costs. Currently, there is no consensus on the best target for imaging in the clinical setting. In humans, our knowledge about the expression of molecular markers within the vasculature is mostly limited to one-time snap shots, for example when analyzing a carotid plaque after a patient had undergone endarterectomy. The kinetics of inflammatory processes in atherosclerosis and in particular the course of expression of potential molecular markers within the inflamed vessel, are yet to be defined. To date, targets that may be most promising for clinical imaging applications comprise adhesion molecules and monocytes/macrophages, as hallmarks of inflammations. Integrins and cell adhesion molecules are not only expressed on the activated endothelium, but also on inflammatory macrophages within the plaque, which should to enable imaging with a good contrast-to noise ratio. Similarly, macrophages are highly abundant within the vulnerable plaque and their presence is moreover clearly associated with the risk of plaque rupture. Macrophages are therefore attractive imaging targets.

Perspectives on Clinical Translation

Our understanding of the inflammatory nature and molecular processes involved in atherosclerosis has substantially advanced over the last 30 years, and it is now widely accepted that inflammation plays a key role in plaque development, maturation and rupture [134]. Molecular imaging, unlike anatomic imaging, is able to elucidate the immunobiological processes inside the vessel wall, otherwise invisible by x-ray, coronary angiography or established intravascular imaging methods. While traditional anatomic imaging modalities have failed to identify the vulnerable plaque that is prone to rupture, it is the aim of ongoing experimental efforts to define imaging modalities that enable the detection and quantification of parameters that can reliably be integrated into clinical diagnostic and therapeutic decision making. In particular, it remains a pressing question in the clinic, which lesion to treat in order to prevent potentially life-threatening complications, such as myocardial infarction and stroke [180, 181]. Molecular imaging is able to translate our advanced knowledge in vascular biology towards these applications. Yet, many hurdles remain to be solved before molecular

imaging platforms can be implemented in routine clinical practice. The lack of probe specificity needs to be overcome by more specific sensors targeting distinct cellular or subcellular processes, and more sensitive detection technologies. Some obstacles, such as the low spatial resolution of nuclear imaging or the restricted penetration depths of near-infrared light, are rooted in physical principles that may not be significantly improved. Modification of the application of these technologies, e.g. imaging via the intravascular route, however, may have the potential to further improve these imaging technologies. First applications of fluorescence imaging in surgical oncology have proven promising when used in cytoreductive surgery [182]. As more and more selective molecular sensors will undergo FDA approval, molecular imaging approaches that have been successful in preclinical animal models will soon be tested in the clinical setting. When the discussed novel imaging platforms are considered for clinical translation, radiation exposure will become a key issue. Although costs of these new imaging technologies are still immense, these may still be modest when compared to the general healthcare costs that arise from the treatment of vascular complications such as myocardial infarction or stroke. Identifying these previously silent culprit lesions before myocardial infarction or stroke occur is a major task for molecular imaging.

When envisioning successful implementation of molecular imaging into daily patient care in the future, one could imagine the following scenario: A patient presents to the emergency room with acute chest pain. The laboratory values as well as the echocardiographic findings point toward an acute coronary syndrome. The patient is therefore brought to the catheterization laboratory for invasive angiography. In addition to the regular x-ray angiogram for detecting vessel obstructions, intravascular fluorescence imaging is performed to screen the entire coronary vascular tree for possible vulnerable plaques, which are not identified by conventional coronary angiography but may nevertheless cause subsequent infarctions within the near future. After angioplasty of an obstructed artery segment the patient is placed on an anti-inflammatory therapeutic regimen. The treatment success can be subsequently monitored non-invasively, either by hybrid PET-CT/PET-MRI or by molecular MRI alone and can guide further therapeutic triage. One could imagine that in parallel, patients would be subjected to genomic risk analysis to guide the aggressiveness of the anti-inflammatory regimen and determine the frequency of follow-up examinations by molecular imaging. Although such implementation of molecular imaging in the clinical routine is appealing, many hurdles, as outlined above,

still need to be overcome [45].

As a concluding remark, the cardiovascular field may benefit from the cancer community where imaging of biomarkers has found its ways into standard daily patient care and is utilized in large clinical trials [45]. In our pursuit of establishing personalized medicine for improving patient care, molecular imaging tools will be of great value for helping physicians to identify vulnerable plaques and triage tailored treatment approaches in individual patients with the aim to avert serious complications of atherosclerosis.

Competing Interests

The authors have declared that no competing interest exists.

References

1. Camici PG, Rimoldi OE, Gaemperli O, Libby P. Non-invasive anatomic and functional imaging of vascular inflammation and unstable plaque. European heart journal. 2012; 33: 1309-17. doi:10.1093/eurheartj/ehs067.
2. Pelisek J, Eckstein HH, Zernecke A. Pathophysiological mechanisms of carotid plaque vulnerability: impact on ischemic stroke. Archivum immunologiae et therapiae experimentalis. 2012; 60: 431-42. doi:10.1007/s00005-012-0192-z.
3. Weber C, Noels H. Atherosclerosis: current pathogenesis and therapeutic options. Nature medicine. 2011; 17: 1410-22. doi:10.1038/nm.2538.
4. Weber C, Zernecke A, Libby P. The multifaceted contributions of leukocyte subsets to atherosclerosis: lessons from mouse models. Nature reviews Immunology. 2008; 8: 802-15. doi:10.1038/nri2415.
5. Leuschner F, Nahrendorf M. Molecular imaging of coronary atherosclerosis and myocardial infarction: considerations for the bench and perspectives for the clinic. Circulation research. 2011; 108: 593-606. doi:10.1161/CIRCRESAHA.110.232678.
6. Quillard T, Libby P. Molecular imaging of atherosclerosis for improving diagnostic and therapeutic development. Circulation research. 2012; 111: 231-44. doi:10.1161/CIRCRESAHA.112.268144.
7. Kajander S, Joutsiniemi E, Saraste M, Pietila M, Ukkonen H, Saraste A, et al. Cardiac positron emission tomography/computed tomography imaging accurately detects anatomically and functionally significant coronary artery disease. Circulation. 2010; 122: 603-13. doi:10.1161/CIRCULATIONAHA.109.915009.
8. Aikawa M, Libby P. The vulnerable atherosclerotic plaque: pathogenesis and therapeutic approach. Cardiovascular pathology. 2004; 13: 125-38. doi:10.1016/S1054-8807(04)00004-3.
9. Casscells W, Naghavi M, Willerson JT. Vulnerable atherosclerotic plaque: a multifocal disease. Circulation. 2003; 107: 2072-5. doi:10.1161/01.CIR.0000069329.70061.68.
10. Naghavi M, Libby P, Falk E, Casscells SW, Litovsky S, Rumberger J, et al. From vulnerable plaque to vulnerable patient: a call for new definitions and risk assessment strategies: Part II. Circulation. 2003; 108: 1772-8. doi:10.1161/01.CIR.0000087481.55887.C9.
11. Naghavi M, Libby P, Falk E, Casscells SW, Litovsky S, Rumberger J, et al. From vulnerable plaque to vulnerable patient: a call for new definitions and risk assessment strategies: Part I. Circulation. 2003; 108: 1664-72. doi:10.1161/01.CIR.0000087480.94275.97.
12. Hyafil F, Cornily JC, Feig JE, Gordon R, Vucic E, Amirbekian V, et al. Noninvasive detection of macrophages using a nanoparticulate contrast agent for computed tomography. Nature medicine. 2007; 13: 636-41. doi:10.1038/nm1571.
13. Luo T, Huang P, Gao G, Shen G, Fu S, Cui D, et al. Mesoporous silica-coated gold nanorods with embedded indocyanine green for dual mode X-ray CT and NIR fluorescence imaging. Optics express. 2011; 19: 17030-9. doi:10.1364/OE.19.017030.
14. Sun H, Yuan Q, Zhang B, Ai K, Zhang P, Lu L. Gd(III) functionalized gold nanorods for multimodal imaging applications. Nanoscale. 2011; 3: 1990-6. doi:10.1039/c0nr00929f.
15. Xiao Y, Hong H, Matson VZ, Javadi A, Xu W, Yang Y, et al. Gold Nanorods Conjugated with Doxorubicin and cRGD for Combined Anticancer Drug Delivery and PET Imaging. Theranostics. 2012; 2: 757-68. doi:10.7150/thno.4756.
16. Esposito L, Saam T, Heider P, Bockelbrink A, Pelisek J, Sepp D, et al. MRI plaque imaging reveals high-risk carotid plaques especially in diabetic patients irrespective of the degree of stenosis. BMC medical imaging. 2010; 10: 27. doi:10.1186/1471-2342-10-27.
17. Saam T, Underhill HR, Chu B, Takaya N, Cai J, Polissar NL, et al. Prevalence of American Heart Association type VI carotid atherosclerotic lesions identified by magnetic resonance imaging for different levels of stenosis as measured by duplex ultrasound. Journal of the American College of Cardiology. 2008; 51: 1014-21. doi:10.1016/j.jacc.2007.10.054.
18. Burtea C, Laurent S, Vander Elst L, Muller RN. Contrast agents: magnetic resonance. Handbook of experimental pharmacology. 2008;: 135-65. doi:10.1007/978-3-540-72718-7_7.
19. Hyafil F, Laissy JP, Mazighi M, Tchetche D, Louedec L, Adle-Biassette H, et al. Ferumoxtran-10-enhanced MRI of the hypercholesterolemic rabbit aorta: relationship between signal loss and macrophage infiltration. Arteriosclerosis, thrombosis, and vascular biology. 2006; 26: 176-81. doi:10.1161/01.ATV.0000194098.82677.57.
20. Korosoglou G, Weiss RG, Kedziorek DA, Walczak P, Gilson WD, Schar M, et al. Noninvasive detection of macrophage-rich atherosclerotic plaque in hyperlipidemic rabbits using "positive contrast" magnetic resonance imaging. Journal of the American College of Cardiology. 2008; 52: 483-91. doi:10.1016/j.jacc.2008.03.063.
21. Morishige K, Kacher DF, Libby P, Josephson L, Ganz P, Weissleder R, et al. High-resolution magnetic resonance imaging enhanced with superparamagnetic nanoparticles measures macrophage burden in atherosclerosis. Circulation. 2010; 122: 1707-15. doi:10.1161/CIRCULATIONAHA.109.891804.
22. Ruehm SG, Corot C, Vogt P, Kolb S, Debatin JF. Magnetic resonance imaging of atherosclerotic plaque with ultrasmall superparamagnetic particles of iron oxide in hyperlipidemic rabbits. Circulation. 2001; 103: 415-22.
23. Trivedi RA, JM UK-I, Graves MJ, Cross JJ, Horsley J, Goddard MJ, et al. In vivo detection of macrophages in human carotid atheroma: temporal dependence of ultrasmall superparamagnetic particles of iron oxide-enhanced MRI. Stroke, a journal of cerebral circulation. 2004; 35: 1631-5. doi:10.1161/01.STR.0000131268.50418.b7.
24. Amirbekian V, Lipinski MJ, Briley-Saebo KC, Amirbekian S, Aguinaldo JG, Weinreb DB, et al. Detecting and assessing macrophages in vivo to evaluate atherosclerosis noninvasively using molecular MRI. Proceedings of the National Academy of Sciences of the United States of America. 2007; 104: 961-6. doi:10.1073/pnas.0606281104.
25. den Adel B, van der Graaf LM, Que I, Strijkers GJ, Lowik CW, Poelmann RE, et al. Contrast enhancement by lipid-based MRI contrast agents in mouse atherosclerotic plaques; a longitudinal study. Contrast media & molecular imaging. 2013; 8: 63-71. doi:10.1002/cmmi.1496.
26. Chen JW, Pham W, Weissleder R, Bogdanov A, Jr. Human myeloperoxidase: a potential target for molecular MR imaging in atherosclerosis. Magnetic resonance in medicine. 2004; 52: 1021-8. doi:10.1002/mrm.20270.
27. Chen JW, Querol Sans M, Bogdanov A, Jr., Weissleder R. Imaging of myeloperoxidase in mice by using novel amplifiable paramagnetic substrates. Radiology. 2006; 240: 473-81. doi:10.1148/radiol.2402050994.
28. Kiessling F, Fokong S, Koczera P, Lederle W, Lammers T. Ultrasound microbubbles for molecular diagnosis, therapy, and theranostics. Journal of nuclear medicine. 2012; 53: 345-8. doi:10.2967/jnumed.111.099754.
29. Ferrante EA, Pickard JE, Rychak J, Klibanov A, Ley K. Dual targeting improves microbubble contrast agent adhesion to VCAM-1 and P-selectin under flow. Journal of controlled release. 2009; 140: 100-7. doi:10.1016/j.jconrel.2009.08.001.
30. Kaufmann BA, Carr CL, Belcik JT, Xie A, Yue Q, Chadderdon S, et al. Molecular imaging of the initial inflammatory response in atherosclerosis: implications for early detection of disease. Arteriosclerosis, thrombosis, and vascular biology. 2010; 30: 54-9. doi:10.1161/ATVBAHA.109.196386.
31. Wu J, Leong-Poi H, Bin J, Yang L, Liao Y, Liu Y, et al. Efficacy of contrast-enhanced US and magnetic microbubbles targeted to vascular cell adhesion molecule-1 for molecular imaging of atherosclerosis. Radiology. 2011; 260: 463-71. doi:10.1148/radiol.11102251.
32. Yang H, Xiong X, Zhang L, Wu C, Liu Y. Adhesion of bio-functionalized ultrasound microbubbles to endothelial cells by targeting to vascular cell adhesion molecule-1 under shear flow. International journal of nanomedicine. 2011; 6: 2043-51. doi:10.2147/IJN.S24808.
33. Wang Y, Zhou J, Zhang Y, Wang X, Chen J. Delivery of TFPI-2 using SonoVue and adenovirus results in the suppression of thrombosis and arterial re-stenosis. Experimental biology and medicine. 2010; 235: 1072-81. doi:10.1258/ebm.2010.010046.
34. Lindner JR. Molecular imaging of myocardial and vascular disorders with ultrasound. JACC Cardiovascular imaging. 2010; 3: 204-11. doi:10.1016/j.jcmg.2009.09.021.
35. Hilderbrand SA, Weissleder R. Near-infrared fluorescence: application to in vivo molecular imaging. Current opinion in chemical biology. 2010; 14: 71-9. doi:10.1016/j.cbpa.2009.09.029.
36. Ntziachristos V, Bremer C, Weissleder R. Fluorescence imaging with near-infrared light: new technological advances that enable in vivo molecular imaging. European radiology. 2003; 13: 195-208. doi:10.1007/s00330-002-1524-x.
37. Ntziachristos V, Razansky D. Molecular imaging by means of multispectral optoacoustic tomography (MSOT). Chemical reviews. 2010; 110: 2783-94. doi:10.1021/cr9002566.
38. Ntziachristos V, Ripoll J, Wang LV, Weissleder R. Looking and listening to light: the evolution of whole-body photonic imaging. Nature biotechnology. 2005; 23: 313-20. doi:10.1038/nbt1074.

39. Ntziachristos V, Tung CH, Bremer C, Weissleder R. Fluorescence molecular tomography resolves protease activity in vivo. Nature medicine. 2002; 8: 757-60. doi:10.1038/nm729.

40. Nahrendorf M, Sosnovik DE, Waterman P, Swirski FK, Pande AN, Aikawa E, et al. Dual channel optical tomographic imaging of leukocyte recruitment and protease activity in the healing myocardial infarct. Circulation research. 2007; 100: 1218-25. doi:10.1161/01.RES.0000265064.46075.31.

41. Nahrendorf M, Waterman P, Thurber G, Groves K, Rajopadhye M, Panizzi P, et al. Hybrid in vivo FMT-CT imaging of protease activity in atherosclerosis with customized nanosensors. Arteriosclerosis, thrombosis, and vascular biology. 2009; 29: 1444-51. doi:10.1161/ATVBAHA.109.193086.

42. Aikawa E, Nahrendorf M, Figueiredo JL, Swirski FK, Shtatland T, Kohler RH, et al. Osteogenesis associates with inflammation in early-stage atherosclerosis evaluated by molecular imaging in vivo. Circulation. 2007; 116: 2841-50. doi:10.1161/CIRCULATIONAHA.107.732867.

43. Aikawa E, Nahrendorf M, Sosnovik D, Lok VM, Jaffer FA, Aikawa M, et al. Multimodality molecular imaging identifies proteolytic and osteogenic activities in early aortic valve disease. Circulation. 2007; 115: 377-86. doi:10.1161/CIRCULATIONAHA.106.654913.

44. von Wallbrunn A, Holtke C, Zuhlsdorf M, Heindel W, Schafers M, Bremer C. In vivo imaging of integrin alpha v beta 3 expression using fluorescence-mediated tomography. European journal of nuclear medicine and molecular imaging. 2007; 34: 745-54. doi:10.1007/s00259-006-0269-1.

45. Weissleder R, Pittet MJ. Imaging in the era of molecular oncology. Nature. 2008; 452: 580-9. doi:10.1038/nature06917.

46. Bremer C, Ntziachristos V, Weissleder R. Optical-based molecular imaging: contrast agents and potential medical applications. European radiology. 2003; 13: 231-43. doi:10.1007/s00330-002-1610-0.

47. Christen T, Nahrendorf M, Wildgruber M, Swirski FK, Aikawa E, Waterman P, et al. Molecular imaging of innate immune cell function in transplant rejection. Circulation. 2009; 119: 1925-32. doi:10.1161/CIRCULATIONAHA.108.796888.

48. Grimm J, Kirsch DG, Windsor SD, Kim CF, Santiago PM, Ntziachristos V, et al. Use of gene expression profiling to direct in vivo molecular imaging of lung cancer. Proceedings of the National Academy of Sciences of the United States of America. 2005; 102: 14404-9. doi:10.1073/pnas.0503920102.

49. Freyer M, Ale A, Schulz RB, Zientkowska M, Ntziachristos V, Englmeier KH. Fast automatic segmentation of anatomical structures in x-ray computed tomography images to improve fluorescence molecular tomography reconstruction. Journal of biomedical optics. 2010; 15: 036006. doi:10.1117/1.3431101.

50. Ale A, Ermolayev V, Herzog E, Cohrs C, de Angelis MH, Ntziachristos V. FMT-XCT: in vivo animal studies with hybrid fluorescence molecular tomography-X-ray computed tomography. Nature methods. 2012; 9: 615-20. doi:10.1038/nmeth.2014.

51. Ale A, Schulz RB, Sarantopoulos A, Ntziachristos V. Imaging performance of a hybrid x-ray computed tomography-fluorescence molecular tomography system using priors. Medical physics. 2010; 37: 1976-86.

52. Schulz RB, Ale A, Sarantopoulos A, Freyer M, Soehngen E, Zientkowska M, et al. Hybrid system for simultaneous fluorescence and x-ray computed tomography. IEEE transactions on medical imaging. 2010; 29: 465-73. doi:10.1109/TMI.2009.2035310.

53. Sarantopoulos A, Themelis G, Ntziachristos V. Imaging the bio-distribution of fluorescent probes using multispectral epi-illumination cryoslicing imaging. Molecular imaging and biology. 2011; 13: 874-85. doi:10.1007/s11307-010-0416-8.

54. Razansky D, Distel M, Vinegoni C, Ma R, Perrimon N, Köster RW, et al. Multispectral opto-acoustic tomography of deep-seated fluorescent proteins in vivo. Nature Photonics. 2009; 3: 412-7. doi:10.1038/nphoton.2009.98.

55. Razansky D, Harlaar NJ, Hillebrands JL, Taruttis A, Herzog E, Zeebregts CJ, et al. Multispectral optoacoustic tomography of matrix metalloproteinase activity in vulnerable human carotid plaques. Molecular imaging and biology. 2012; 14: 277-85. doi:10.1007/s11307-011-0502-6.

56. Nair A, Kuban BD, Obuchowski N, Vince DG. Assessing spectral algorithms to predict atherosclerotic plaque composition with normalized and raw intravascular ultrasound data. Ultrasound in medicine & biology. 2001; 27: 1319-31.

57. Nair A, Kuban BD, Tuzcu EM, Schoenhagen P, Nissen SE, Vince DG. Coronary plaque classification with intravascular ultrasound radiofrequency data analysis. Circulation. 2002; 106: 2200-6.

58. Jang IK, Bouma BE, Kang DH, Park SJ, Park SW, Seung KB, et al. Visualization of coronary atherosclerotic plaques in patients using optical coherence tomography: comparison with intravascular ultrasound. Journal of the American College of Cardiology. 2002; 39: 604-9.

59. Jang IK, Tearney GJ, MacNeill B, Takano M, Moselewski F, Iftima N, et al. In vivo characterization of coronary atherosclerotic plaque by use of optical coherence tomography. Circulation. 2005; 111: 1551-5. doi:10.1161/01.CIR.0000159354.43778.69.

60. Serruys PW, Ormiston JA, Onuma Y, Regar E, Gonzalo N, Garcia-Garcia HM, et al. A bioabsorbable everolimus-eluting coronary stent system (ABSORB): 2-year outcomes and results from multiple imaging methods. Lancet. 2009; 373: 897-910. doi:10.1016/S0140-6736(09)60325-1.

61. Maehara A, Mintz GS, Weissman NJ. Advances in intravascular imaging. Circulation Cardiovascular interventions. 2009; 2: 482-90. doi:10.1161/CIRCINTERVENTIONS.109.868398.

62. Hosokawa R, Kambara N, Ohba M, Mukai T, Ogawa M, Motomura H, et al. A catheter-based intravascular radiation detector of vulnerable plaques. Journal of nuclear medicine. 2006; 47: 863-7.

63. Lederman RJ, Raylman RR, Fisher SJ, Kison PV, San H, Nabel EG, et al. Detection of atherosclerosis using a novel positron-sensitive probe and 18-fluorodeoxyglucose (FDG). Nuclear medicine communications. 2001; 22: 747-53.

64. Strauss HW, Mari C, Patt BE, Ghazarossian V. Intravascular radiation detectors for the detection of vulnerable atheroma. Journal of the American College of Cardiology. 2006; 47: C97-100. doi:10.1016/j.jacc.2005.11.051.

65. Jaffer FA, Vinegoni C, John MC, Aikawa E, Gold HK, Finn AV, et al. Real-time catheter molecular sensing of inflammation in proteolytically active atherosclerosis. Circulation. 2008; 118: 1802-9. doi:10.1161/CIRCULATIONAHA.108.785881.

66. Jaffer FA, Calfon MA, Rosenthal A, Mallas G, Razansky RN, Mauskapf A, et al. Two-dimensional intravascular near-infrared fluorescence molecular imaging of inflammation in atherosclerosis and stent-induced vascular injury. Journal of the American College of Cardiology. 2011; 57: 2516-26. doi:10.1016/j.jacc.2011.02.036.

67. Yoo H, Kim JW, Shishkov M, Namati E, Morse T, Shubochkin R, et al. Intra-arterial catheter for simultaneous microstructural and molecular imaging in vivo. Nature medicine. 2011; 17: 1680-4. doi:10.1038/nm.2555.

68. Rosenthal A, Jaffer FA, Ntziachristos V. Intravascular multispectral optoacoustic tomography of atherosclerosis: prospects and challenges. Imaging in medicine. 2012; 4: 299-310. doi:10.2217/iim.12.20.

69. Chiu JJ, Chien S. Effects of disturbed flow on vascular endothelium: pathophysiological basis and clinical perspectives. Physiological reviews. 2011; 91: 327-87. doi:10.1152/physrev.00047.2009.

70. Zhou J, Lee PL, Tsai CS, Lee CI, Yang TL, Chuang HS, et al. Force-specific activation of Smad1/5 regulates vascular endothelial cell cycle progression in response to disturbed flow. Proceedings of the National Academy of Sciences of the United States of America. 2012; 109: 7770-5. doi:10.1073/pnas.1205476109.

71. Hahn C, Schwartz MA. The role of cellular adaptation to mechanical forces in atherosclerosis. Arteriosclerosis, thrombosis, and vascular biology. 2008; 28: 2101-7. doi:10.1161/ATVBAHA.108.165951.

72. Lehoux S. Redox signalling in vascular responses to shear and stretch. Cardiovascular research. 2006; 71: 269-79. doi:10.1016/j.cardiores.2006.05.008.

73. Miyazaki T, Taketomi Y, Takimoto M, Lei XF, Arita S, Kim-Kaneyama JR, et al. m-Calpain induction in vascular endothelial cells on human and mouse atheromas and its roles in VE-cadherin disorganization and atherosclerosis. Circulation. 2011; 124: 2522-32. doi:10.1161/CIRCULATIONAHA.111.021675.

74. Kerwin WS, Canton G. Advanced techniques for MRI of atherosclerotic plaque. Topics in magnetic resonance imaging : TMRI. 2009; 20: 217-25. doi:10.1097/RMR.0b013e3181ea2853.

75. Ley K, Laudanna C, Cybulsky MI, Nourshargh S. Getting to the site of inflammation: the leukocyte adhesion cascade updated. Nature reviews Immunology. 2007; 7: 678-89. doi:10.1038/nri2156.

76. Broisat A, Riou LM, Ardisson V, Boturyn D, Dumy P, Fagret D, et al. Molecular imaging of vascular cell adhesion molecule-1 expression in experimental atherosclerotic plaques with radiolabelled B2702-p. European journal of nuclear medicine and molecular imaging. 2007; 34: 830-40. doi:10.1007/s00259-006-0310-4.

77. Kaufmann BA, Sanders JM, Davis C, Xie A, Aldred P, Sarembock IJ, et al. Molecular imaging of inflammation in atherosclerosis with targeted ultrasound detection of vascular cell adhesion molecule-1. Circulation. 2007; 116: 276-84. doi:10.1161/CIRCULATIONAHA.106.684738.

78. Kelly KA, Allport JR, Tsourkas A, Shinde-Patil VR, Josephson L, Weissleder R. Detection of vascular adhesion molecule-1 expression using a novel multimodal nanoparticle. Circulation research. 2005; 96: 327-36. doi:10.1161/01.RES.0000155722.17881.dd.

79. McAteer MA, Mankia K, Ruparelia N, Jefferson A, Nugent HB, Stork LA, et al. A leukocyte-mimetic magnetic resonance imaging contrast agent homes rapidly to activated endothelium and tracks with atherosclerotic lesion macrophage content. Arteriosclerosis, thrombosis, and vascular biology. 2012; 32: 1427-35. doi:10.1161/ATVBAHA.111.241844.

80. Nahrendorf M, Keliher E, Panizzi P, Zhang H, Hembrador S, Figueiredo JL, et al. 18F-4V for PET-CT imaging of VCAM-1 expression in atherosclerosis. JACC Cardiovascular imaging. 2009; 2: 1213-22. doi:10.1016/j.jcmg.2009.04.016.

81. Nahrendorf M, Zhang H, Hembrador S, Panizzi P, Sosnovik DE, Aikawa E, et al. Nanoparticle PET-CT imaging of macrophages in inflammatory atherosclerosis. Circulation. 2008; 117: 379-87. doi:10.1161/CIRCULATIONAHA.107.741181.

82. Southworth R, Kaneda M, Chen J, Zhang L, Zhang H, Yang X, et al. Renal vascular inflammation induced by Western diet in ApoE-null mice quantified by (19)F NMR of VCAM-1 targeted nanobeacons. Nanomedicine : nanotechnology, biology, and medicine. 2009; 5: 359-67. doi:10.1016/j.nano.2008.12.002.

83. Michalska M, Machtoub L, Manthey HD, Bauer E, Herold V, Krohne G, et al. Visualization of vascular inflammation in the atherosclerotic mouse by ultrasmall superparamagnetic iron oxide vascular cell adhesion molecule-1-specific nanoparticles. Arteriosclerosis, thrombosis, and vascular biology. 2012; 32: 2350-7. doi:10.1161/ATVBAHA.112.255224.

84. Kelly KA, Nahrendorf M, Yu AM, Reynolds F, Weissleder R. In vivo phage display selection yields atherosclerotic plaque targeted peptides for imaging. Molecular imaging and biology. 2006; 8: 201-7. doi:10.1007/s11307-006-0043-6.

85. Nahrendorf M, Jaffer FA, Kelly KA, Sosnovik DE, Aikawa E, Libby P, et al. Noninvasive vascular cell adhesion molecule-1 imaging identifies inflammatory activation of cells in atherosclerosis. Circulation. 2006; 114: 1504-11. doi:10.1161/CIRCULATIONAHA.106.646380.

86. Jefferson A, Wijesurendra RS, McAteer MA, Digby JE, Douglas G, Bannister T, et al. Molecular imaging with optical coherence tomography using ligand-conjugated microparticles that detect activated endothelial cells: rational design through target quantification. Atherosclerosis. 2011; 219: 579-87. doi:10.1016/j.atherosclerosis.2011.07.127.

87. McAteer MA, Schneider JE, Ali ZA, Warrick N, Bursill CA, von zur Muhlen C, et al. Magnetic resonance imaging of endothelial adhesion molecules in mouse atherosclerosis using dual-targeted microparticles of iron oxide. Arteriosclerosis, thrombosis, and vascular biology. 2008; 28: 77-83. doi:10.1161/ATVBAHA.107.145466.

88. Paulis LE, Jacobs I, van de Akker N, Geelen T, Molin D, Starmans LW, et al. Targeting of ICAM-1 on vascular endothelium under static and shear stress conditions using a liposomal Gd-based MRI contrast agent. Journal of nanobiotechnology. 2012; 10: 25. doi:10.1186/1477-3155-10-25.

89. Villanueva FS, Jankowski RJ, Klibanov S, Pina ML, Alber SM, Watkins SC, et al. Microbubbles targeted to intercellular adhesion molecule-1 bind to activated coronary artery endothelial cells. Circulation. 1998; 98: 1-5.

90. Taruttis A, Wildgruber M, Kosanke K, Beziere N, Licha K, Haag R, et al. Multispectral optoacoustic tomography of myocardial infarction. Photoacoustics. 2012; doi:10.1016/j.pacs.2012.11.001.

91. Dernedde J, Rausch A, Weinhart M, Enders S, Tauber R, Licha K, et al. Dendritic polyglycerol sulfates as multivalent inhibitors of inflammation. Proceedings of the National Academy of Sciences of the United States of America. 2010; 107: 19679-84. doi:10.1073/pnas.1003103107.

92. Pedersen SF, Thrysoe SA, Paaske WP, Thim T, Falk E, Ringgaard S, et al. CMR assessment of endothelial damage and angiogenesis in porcine coronary arteries using gadofosveset. Journal of cardiovascular magnetic resonance. 2011; 13: 10. doi:10.1186/1532-429X-13-10.

93. Phinikaridou A, Andia ME, Protti A, Indermuehle A, Shah A, Smith A, et al. Noninvasive magnetic resonance imaging evaluation of endothelial permeability in murine atherosclerosis using an albumin-binding contrast agent. Circulation. 2012; 126: 707-19. doi:10.1161/CIRCULATIONAHA.112.092098.

94. Vinegoni C, Botnaru I, Aikawa E, Calfon MA, Iwamoto Y, Folco EJ, et al. Indocyanine green enables near-infrared fluorescence imaging of lipid-rich, inflamed atherosclerotic plaques. Science translational medicine. 2011; 3: 84ra45. doi:10.1126/scitranslmed.3001577.

95. Hansson GK, Libby P. The immune response in atherosclerosis: a double-edged sword. Nature reviews Immunology. 2006; 6: 508-19. doi:10.1038/nri1882.

96. Swirski FK, Weissleder R, Pittet MJ. Heterogeneous in vivo behavior of monocyte subsets in atherosclerosis. Arteriosclerosis, thrombosis, and vascular biology. 2009; 29: 1424-32. doi:10.1161/ATVBAHA.108.180521.

97. Gordon S, Taylor PR. Monocyte and macrophage heterogeneity. Nature reviews Immunology. 2005; 5: 953-64. doi:10.1038/nri1733.

98. Robbins CS, Chudnovskiy A, Rauch PJ, Figueiredo JL, Iwamoto Y, Gorbatov R, et al. Extramedullary hematopoiesis generates Ly-6C(high) monocytes that infiltrate atherosclerotic lesions. Circulation. 2012; 125: 364-74. doi:10.1161/CIRCULATIONAHA.111.061986.

99. Swirski FK, Libby P, Aikawa E, Alcaide P, Luscinskas FW, Weissleder R, et al. Ly-6Chi monocytes dominate hypercholesterolemia-associated monocytosis and give rise to macrophages in atheromata. The Journal of clinical investigation. 2007; 117: 195-205. doi:10.1172/JCI29950.

100. Schlitt A, Heine GH, Blankenberg S, Espinola-Klein C, Dopheide JF, Bickel C, et al. CD14+CD16+ monocytes in coronary artery disease and their relationship to serum TNF-alpha levels. Thrombosis and haemostasis. 2004; 92: 419-24. doi:10.1267/THRO04080419.

101. Wildgruber M, Lee H, Chudnovskiy A, Yoon TJ, Etzrodt M, Pittet MJ, et al. Monocyte subset dynamics in human atherosclerosis can be profiled with magnetic nano-sensors. PloS one. 2009; 4: e5663. doi:10.1371/journal.pone.0005663.

102. Tsujioka H, Imanishi T, Ikejima H, Kuroi A, Takarada S, Tanimoto T, et al. Impact of heterogeneity of human peripheral blood monocyte subsets on myocardial salvage in patients with primary acute myocardial infarction. Journal of the American College of Cardiology. 2009; 54: 130-8. doi:10.1016/j.jacc.2009.04.021.

103. Tang TY, Howarth SP, Miller SR, Graves MJ, Patterson AJ, JM UK-I, et al. The ATHEROMA (Atorvastatin Therapy: Effects on Reduction of Macrophage Activity) Study. Evaluation using ultrasmall superparamagnetic iron oxide-enhanced magnetic resonance imaging in carotid disease. Journal of the American College of Cardiology. 2009; 53: 2039-50. doi:10.1016/j.jacc.2009.03.018.

104. Nahrendorf M, Swirski FK, Aikawa E, Stangenberg L, Wurdinger T, Figueiredo JL, et al. The healing myocardium sequentially mobilizes two monocyte subsets with divergent and complementary functions. The Journal of experimental medicine. 2007; 204: 3037-47. doi:10.1084/jem.20070885.

105. Settles M, Etzrodt M, Kosanke K, Schiemann M, Zimmermann A, Meier R, et al. Different capacity of monocyte subsets to phagocytose iron-oxide nanoparticles. PloS one. 2011; 6: e25197. doi:10.1371/journal.pone.0025197.

106. Makowski MR, Varma G, Wiethoff AJ, Smith A, Mattock K, Jansen CH, et al. Noninvasive assessment of atherosclerotic plaque progression in ApoE-/- mice using susceptibility gradient mapping. Circulation Cardiovascular imaging. 2011; 4: 295-303. doi:10.1161/CIRCIMAGING.110.957209.

107. Metz S, Beer AJ, Settles M, Pelisek J, Botnar RM, Rummeny EJ, et al. Characterization of carotid artery plaques with USPIO-enhanced MRI: assessment of inflammation and vascularity as in vivo imaging biomarkers for plaque vulnerability. The international journal of cardiovascular imaging. 2011; 27: 901-12. doi:10.1007/s10554-010-9736-7.

108. Schmitz SA, Coupland SE, Gust R, Winterhalter S, Wagner S, Kresse M, et al. Superparamagnetic iron oxide-enhanced MRI of atherosclerotic plaques in Watanabe hereditable hyperlipidemic rabbits. Investigative radiology. 2000; 35: 460-71.

109. de Vries IJ, Lesterhuis WJ, Barentsz JO, Verdijk P, van Krieken JH, Boerman OC, et al. Magnetic resonance tracking of dendritic cells in melanoma patients for monitoring of cellular therapy. Nature biotechnology. 2005; 23: 1407-13. doi:10.1038/nbt1154.

110. Kircher MF, Grimm J, Swirski FK, Libby P, Gerszten RE, Allport JR, et al. Noninvasive in vivo imaging of monocyte trafficking to atherosclerotic lesions. Circulation. 2008; 117: 388-95. doi:10.1161/CIRCULATIONAHA.107.719765.

111. Mulder WJ, Strijkers GJ, Briley-Saboe KC, Frias JC, Aguinaldo JG, Vucic E, et al. Molecular imaging of macrophages in atherosclerotic plaques using bimodal PEG-micelles. Magnetic resonance in medicine. 2007; 58: 1164-70. doi:10.1002/mrm.21315.

112. te Boekhorst BC, Bovens SM, Hellings WE, van der Kraak PH, van de Kolk KW, Vink A, et al. Molecular MRI of murine atherosclerotic plaque targeting NGAL: a protein associated with unstable human plaque characteristics. Cardiovascular research. 2011; 89: 680-8. doi:10.1093/cvr/cvq340.

113. te Boekhorst BC, Bovens SM, Rodrigues-Feo J, Sanders HM, van de Kolk CW, de Kroon AI, et al. Characterization and in vitro and in vivo testing of CB2-receptor- and NGAL-targeted paramagnetic micelles for molecular MRI of vulnerable atherosclerotic plaque. Molecular imaging and biology. 2010; 12: 635-51. doi:10.1007/s11307-010-0323-z.

114. Laitinen I, Saraste A, Weidl E, Poethko T, Weber AW, Nekolla SG, et al. Evaluation of alphavbeta3 integrin-targeted positron emission tomography tracer 18F-galacto-RGD for imaging of vascular inflammation in atherosclerotic mice. Circulation Cardiovascular imaging. 2009; 2: 331-8. doi:10.1161/CIRCIMAGING.108.846865.

115. Saraste A, Laitinen I, Weidl E, Wildgruber M, Weber AW, Nekolla SG, et al. Diet intervention reduces uptake of alphavbeta3 integrin-targeted PET tracer 18F-galacto-RGD in mouse atherosclerotic plaques. Journal of nuclear cardiology. 2012; 19: 775-84. doi:10.1007/s12350-012-9554-5.

116. Burtea C, Laurent S, Murariu O, Rattat D, Toubeau G, Verbruggen A, et al. Molecular imaging of alpha v beta3 integrin expression in atherosclerotic plaques with a mimetic of RGD peptide grafted to Gd-DTPA. Cardiovascular research. 2008; 78: 148-57. doi:10.1093/cvr/cvm115.

117. Calcagno C, Cornily JC, Hyafil F, Rudd JH, Briley-Saebo KC, Mani V, et al. Detection of neovessels in atherosclerotic plaques of rabbits using dynamic contrast enhanced MRI and 18F-FDG PET. Arteriosclerosis, thrombosis, and vascular biology. 2008; 28: 1311-7. doi:10.1161/ATVBAHA.108.166173.

118. Rudd JH, Warburton EA, Fryer TD, Jones HA, Clark JC, Antoun N, et al. Imaging atherosclerotic plaque inflammation with [18F]-fluorodeoxyglucose positron emission tomography. Circulation. 2002; 105: 2708-11.

119. Silvera SS, Aidi HE, Rudd JH, Mani V, Yang L, Farkouh M, et al. Multimodality imaging of atherosclerotic plaque activity and composition using FDG-PET/CT and MRI in carotid and femoral arteries. Atherosclerosis. 2009; 207: 139-43. doi:10.1016/j.atherosclerosis.2009.04.023.

120. Tu C, Ng TS, Sohi HK, Palko HA, House A, Jacobs RE, et al. Receptor-targeted iron oxide nanoparticles for molecular MR imaging of inflamed atherosclerotic plaques. Biomaterials. 2011; 32: 7209-16. doi:10.1016/j.biomaterials.2011.06.026.

121. Bucerius J, Mani V, Moncrieff C, Rudd JH, Machac J, Fuster V, et al. Impact of noninsulin-dependent type 2 diabetes on carotid wall 18F-fluorodeoxyglucose positron emission tomography uptake. Journal of the American College of Cardiology. 2012; 59: 2080-8. doi:10.1016/j.jacc.2011.11.069.

122. Marnane M, Merwick A, Sheehan OC, Hannon N, Foran P, Grant T, et al. Carotid plaque inflammation on 18F-fluorodeoxyglucose positron emission tomography predicts early stroke recurrence. Annals of neurology. 2012; 71: 709-18. doi:10.1002/ana.23553.

123. Moustafa RR, Izquierdo-Garcia D, Fryer TD, Graves MJ, Rudd JH, Gillard JH, et al. Carotid plaque inflammation is associated with cerebral microembolism in patients with recent transient ischemic attack or stroke: a pilot study. Circulation Cardiovascular imaging. 2010; 3: 536-41. doi:10.1161/CIRCIMAGING.110.938225.

124. Fayad ZA, Mani V, Woodward M, Kallend D, Abt M, Burgess T, et al. Safety and efficacy of dalcetrapib on atherosclerotic disease using novel non-invasive multimodality imaging (dal-PLAQUE): a randomised clinical trial. Lancet. 2011; 378: 1547-59. doi:10.1016/S0140-6736(11)61383-4.

125. Pedersen SF, Graebe M, Fisker Hag AM, Hojgaard L, Sillesen H, Kjaer A. Gene expression and 18FDG uptake in atherosclerotic carotid plaques. Nuclear

medicine communications. 2010; 31: 423-9. doi:10.1097/MNM.0b013e32833767e0.

126. Myers KS, Rudd JH, Hailman EP, Bolognese JA, Burke J, Pinto CA, et al. Correlation between arterial FDG uptake and biomarkers in peripheral artery disease. JACC Cardiovascular imaging. 2012; 5: 38-45. doi:10.1016/j.jcmg.2011.08.019.

127. Folco EJ, Sheikine Y, Rocha VZ, Christen T, Shvartz E, Sukhova GK, et al. Hypoxia but not inflammation augments glucose uptake in human macrophages: Implications for imaging atherosclerosis with 18fluorine-labeled 2-deoxy-D-glucose positron emission tomography. Journal of the American College of Cardiology. 2011; 58: 603-14. doi:10.1016/j.jacc.2011.03.044.

128. Briley-Saebo KC, Shaw PX, Mulder WJ, Choi SH, Vucic E, Aguinaldo JG, et al. Targeted molecular probes for imaging atherosclerotic lesions with magnetic resonance using antibodies that recognize oxidation-specific epitopes. Circulation. 2008; 117: 3206-15. doi:10.1161/CIRCULATIONAHA.107.757120.

129. Sugiyama S, Okada Y, Sukhova GK, Virmani R, Heinecke JW, Libby P. Macrophage myeloperoxidase regulation by granulocyte macrophage colony-stimulating factor in human atherosclerosis and implications in acute coronary syndromes. The American journal of pathology. 2001; 158: 879-91. doi:10.1016/S0002-9440(10)64036-9.

130. Nahrendorf M, Sosnovik D, Chen JW, Panizzi P, Figueiredo JL, Aikawa E, et al. Activatable magnetic resonance imaging agent reports myeloperoxidase activity in healing infarcts and noninvasively detects the antiinflammatory effects of atorvastatin on ischemia-reperfusion injury. Circulation. 2008; 117: 1153-60. doi:10.1161/CIRCULATIONAHA.107.756510.

131. Swirski FK, Wildgruber M, Ueno T, Figueiredo JL, Panizzi P, Iwamoto Y, et al. Myeloperoxidase-rich Ly-6C+ myeloid cells infiltrate allografts and contribute to an imaging signature of organ rejection in mice. The Journal of clinical investigation. 2010; 120: 2627-34. doi:10.1172/JCI42304.

132. Ronald JA, Chen JW, Chen Y, Hamilton AM, Rodriguez E, Reynolds F, et al. Enzyme-sensitive magnetic resonance imaging targeting myeloperoxidase identifies active inflammation in experimental rabbit atherosclerotic plaques. Circulation. 2009; 120: 592-9. doi:10.1161/CIRCULATIONAHA.108.813998.

133. Panizzi P, Nahrendorf M, Wildgruber M, Waterman P, Figueiredo JL, Aikawa E, et al. Oxazine conjugated nanoparticle detects in vivo hypochlorous acid and peroxynitrite generation. Journal of the American Chemical Society. 2009; 131: 15739-44. doi:10.1021/ja903922u.

134. Libby P. Inflammation in atherosclerosis. Nature. 2002; 420: 868-74. doi:10.1038/nature01323.

135. Haider N, Hartung D, Fujimoto S, Petrov A, Kolodgie FD, Virmani R, et al. Dual molecular imaging for targeting metalloproteinase activity and apoptosis in atherosclerosis: molecular imaging facilitates understanding of pathogenesis. Journal of nuclear cardiology. 2009; 16: 753-62. doi:10.1007/s12350-009-9107-8.

136. Razavian M, Tavakoli S, Zhang J, Nie L, Dobrucki LW, Sinusas AJ, et al. Atherosclerosis plaque heterogeneity and response to therapy detected by in vivo molecular imaging of matrix metalloproteinase activation. Journal of nuclear medicine. 2011; 52: 1795-802. doi:10.2967/jnumed.111.092379.

137. Quillard T, Croce K, Jaffer FA, Weissleder R, Libby P. Molecular imaging of macrophage protease activity in cardiovascular inflammation in vivo. Thrombosis and haemostasis. 2011; 105: 828-36. doi:10.1160/TH10-09-0589.

138. Deguchi JO, Aikawa M, Tung CH, Aikawa E, Kim DE, Ntziachristos V, et al. Inflammation in atherosclerosis: visualizing matrix metalloproteinase action in macrophages in vivo. Circulation. 2006; 114: 55-62. doi:10.1161/CIRCULATIONAHA.106.619056.

139. Chen J, Tung CH, Mahmood U, Ntziachristos V, Gyurko R, Fishman MC, et al. In vivo imaging of proteolytic activity in atherosclerosis. Circulation. 2002; 105: 2766-71.

140. Kim DE, Kim JY, Schellingerhout D, Shon SM, Jeong SW, Kim EJ, et al. Molecular imaging of cathepsin B proteolytic enzyme activity reflects the inflammatory component of atherosclerotic pathology and can quantitatively demonstrate the antiatherosclerotic therapeutic effects of atorvastatin and glucosamine. Molecular imaging. 2009; 8: 291-301.

141. Jaffer FA, Kim DE, Quinti L, Tung CH, Aikawa E, Pande AN, et al. Optical visualization of cathepsin K activity in atherosclerosis with a novel, protease-activatable fluorescence sensor. Circulation. 2007; 115: 2292-8. doi:10.1161/CIRCULATIONAHA.106.660340.

142. Aikawa E, Aikawa M, Libby P, Figueiredo JL, Rusanescu G, Iwamoto Y, et al. Arterial and aortic valve calcification abolished by elastolytic cathepsin S deficiency in chronic renal disease. Circulation. 2009; 119: 1785-94. doi:10.1161/CIRCULATIONAHA.108.827972.

143. Amirbekian V, Aguinaldo JG, Amirbekian S, Hyafil F, Vucic E, Sirol M, et al. Atherosclerosis and matrix metalloproteinases: experimental molecular MR imaging in vivo. Radiology. 2009; 251: 429-38. doi:10.1148/radiol.2511080539.

144. Hyafil F, Vucic E, Cornily JC, Sharma R, Amirbekian V, Blackwell F, et al. Monitoring of arterial wall remodelling in atherosclerotic rabbits with a magnetic resonance imaging contrast agent binding to matrix metalloproteinases. European heart journal. 2011; 32: 1561-71. doi:10.1093/eurheartj/ehq413.

145. Tabas I. Macrophage apoptosis in atherosclerosis: consequences on plaque progression and the role of endoplasmic reticulum stress. Antioxidants & redox signaling. 2009; 11: 2333-9. doi:10.1089/ARS.2009.2469.

146. Laufer EM, Reutelingsperger CP, Narula J, Hofstra L. Annexin A5: an imaging biomarker of cardiovascular risk. Basic research in cardiology. 2008; 103: 95-104. doi:10.1007/s00395-008-0701-8.

147. Laufer EM, Winkens HM, Corsten MF, Reutelingsperger CP, Narula J, Hofstra L. PET and SPECT imaging of apoptosis in vulnerable atherosclerotic plaques with radiolabeled Annexin A5. The quarterly journal of nuclear medicine and molecular imaging. 2009; 53: 26-34.

148. Ishino S, Kuge Y, Takai N, Tamaki N, Strauss HW, Blankenberg FG, et al. 99mTc-Annexin A5 for noninvasive characterization of atherosclerotic lesions: imaging and histological studies in myocardial infarction-prone Watanabe heritable hyperlipidemic rabbits. European journal of nuclear medicine and molecular imaging. 2007; 34: 889-99. doi:10.1007/s00259-006-0289-x.

149. Isobe S, Tsimikas S, Zhou J, Fujimoto S, Sarai M, Branks MJ, et al. Noninvasive imaging of atherosclerotic lesions in apolipoprotein E-deficient and low-density-lipoprotein receptor-deficient mice with annexin A5. Journal of nuclear medicine : official publication, Society of Nuclear Medicine. 2006; 47: 1497-505.

150. Johnson LL, Schofield L, Donahay T, Narula N, Narula J. 99mTc-annexin V imaging for in vivo detection of atherosclerotic lesions in porcine coronary arteries. Journal of nuclear medicine. 2005; 46: 1186-93.

151. Kietselaer BL, Reutelingsperger CP, Heidendal GA, Daemen MJ, Mess WH, Hofstra L, et al. Noninvasive detection of plaque instability with use of radiolabeled annexin A5 in patients with carotid-artery atherosclerosis. The New England journal of medicine. 2004; 350: 1472-3. doi:10.1056/NEJM200404013501425.

152. Sarai M, Hartung D, Petrov A, Zhou J, Narula N, Hofstra L, et al. Broad and specific caspase inhibitor-induced acute repression of apoptosis in atherosclerotic lesions evaluated by radiolabeled annexin A5 imaging. Journal of the American College of Cardiology. 2007; 50: 2305-12. doi:10.1016/j.jacc.2007.08.044.

153. van Tilborg GA, Vucic E, Strijkers GJ, Cormode DP, Mani V, Skajaa T, et al. Annexin A5-functionalized bimodal nanoparticles for MRI and fluorescence imaging of atherosclerotic plaques. Bioconjugate chemistry. 2010; 21: 1794-803. doi:10.1021/bc100091q.

154. Sosnovik DE, Garanger E, Aikawa E, Nahrendorf M, Figueiredo JL, Dai G, et al. Molecular MRI of cardiomyocyte apoptosis with simultaneous delayed-enhancement MRI distinguishes apoptotic and necrotic myocytes in vivo: potential for midmyocardial salvage in acute ischemia. Circulation Cardiovascular imaging. 2009; 2: 460-7. doi:10.1161/CIRCIMAGING.109.859678.

155. Sosnovik DE, Nahrendorf M, Panizzi P, Matsui T, Aikawa E, Dai G, et al. Molecular MRI detects low levels of cardiomyocyte apoptosis in a transgenic model of chronic heart failure. Circulation Cardiovascular imaging. 2009; 2: 468-75. doi:10.1161/CIRCIMAGING.109.863779.

156. Barkhausen J, Ebert W, Heyer C, Debatin JF, Weinmann HJ. Detection of atherosclerotic plaque with Gadofluorine-enhanced magnetic resonance imaging. Circulation. 2003; 108: 605-9. doi:10.1161/01.CIR.0000079099.36306.10.

157. Meding J, Urich M, Licha K, Reinhardt M, Misselwitz B, Fayad ZA, et al. Magnetic resonance imaging of atherosclerosis by targeting extracellular matrix deposition with Gadofluorine M. Contrast media & molecular imaging. 2007; 2: 120-9. doi:10.1002/cmmi.137.

158. Ronald JA, Chen Y, Belisle AJ, Hamilton AM, Rogers KA, Hegele RA, et al. Comparison of gadofluorine-M and Gd-DTPA for noninvasive staging of atherosclerotic plaque stability using MRI. Circulation Cardiovascular imaging. 2009; 2: 226-34. doi:10.1161/CIRCIMAGING.108.826826.

159. Makowski MR, Wiethoff AJ, Blume U, Cuello F, Warley A, Jansen CH, et al. Assessment of atherosclerotic plaque burden with an elastin-specific magnetic resonance contrast agent. Nature medicine. 2011; 17: 383-8. doi:10.1038/nm.2310.

160. von Bary C, Makowski M, Preissel A, Keithahn A, Warley A, Spuentrup E, et al. MRI of coronary wall remodeling in a swine model of coronary injury using an elastin-binding contrast agent. Circulation Cardiovascular imaging. 2011; 4: 147-55. doi:10.1161/CIRCIMAGING.109.895607.

161. Phinikaridou A, Andia ME, Shah AM, Botnar R. Advances in Molecular Imaging of Atherosclerosis and Myocardial Infarction: Shedding New Light on *In vivo* Cardiovascular Biology. American journal of physiology Heart and circulatory physiology. 2012. doi:10.1152/ajpheart.00583.2012.

162. Sanders HM, Strijkers GJ, Mulder WJ, Huinink HP, Erich SJ, Adan OC, et al. Morphology, binding behavior and MR-properties of paramagnetic collagen-binding liposomes. Contrast media & molecular imaging. 2009; 4: 81-8. doi:10.1002/cmmi.266.

163. Alexopoulos N, Raggi P. Calcification in atherosclerosis. Nature reviews Cardiology. 2009; 6: 681-8. doi:10.1038/nrcardio.2009.165.

164. Dweck MR, Jones C, Joshi NV, Fletcher AM, Richardson H, White A, et al. Assessment of valvular calcification and inflammation by positron emission tomography in patients with aortic stenosis. Circulation. 2012; 125: 76-86. doi:10.1161/CIRCULATIONAHA.111.051052.

165. Hjortnaes J, Butcher J, Figueiredo JL, Riccio M, Kohler RH, Kozloff KM, et al. Arterial and aortic valve calcification inversely correlates with osteoporotic bone remodelling: a role for inflammation. European heart journal. 2010; 31: 1975-84. doi:10.1093/eurheartj/ehq237.

166. Motoyama S, Kondo T, Sarai M, Sugiura A, Harigaya H, Sato T, et al. Multislice computed tomographic characteristics of coronary lesions in acute

coronary syndromes. Journal of the American College of Cardiology. 2007; 50: 319-26. doi:10.1016/j.jacc.2007.03.044.

167. Duerschmied D, Meissner M, Peter K, Neudorfer I, Roming F, Zirlik A, et al. Molecular magnetic resonance imaging allows the detection of activated platelets in a new mouse model of coronary artery thrombosis. Investigative radiology. 2011; 46: 618-23. doi:10.1097/RLI.0b013e31821e62fb.

168. von zur Muhlen C, Peter K, Ali ZA, Schneider JE, McAteer MA, Neubauer S, et al. Visualization of activated platelets by targeted magnetic resonance imaging utilizing conformation-specific antibodies against glycoprotein IIb/IIIa. Journal of vascular research. 2009; 46: 6-14. doi:10.1159/000135660.

169. Botnar RM, Buecker A, Wiethoff AJ, Parsons EC, Jr., Katoh M, Katsimaglis G, et al. In vivo magnetic resonance imaging of coronary thrombosis using a fibrin-binding molecular magnetic resonance contrast agent. Circulation. 2004; 110: 1463-6. doi:10.1161/01.CIR.0000134960.31304.87.

170. Botnar RM, Perez AS, Witte S, Wiethoff AJ, Laredo J, Hamilton J, et al. In vivo molecular imaging of acute and subacute thrombosis using a fibrin-binding magnetic resonance imaging contrast agent. Circulation. 2004; 109: 2023-9. doi:10.1161/01.CIR.0000127034.50006.C0.

171. Spuentrup E, Buecker A, Katoh M, Wiethoff AJ, Parsons EC, Jr., Botnar RM, et al. Molecular magnetic resonance imaging of coronary thrombosis and pulmonary emboli with a novel fibrin-targeted contrast agent. Circulation. 2005; 111: 1377-82. doi:10.1161/01.CIR.0000158478.29668.9B.

172. Spuentrup E, Fausten B, Kinzel S, Wiethoff AJ, Botnar RM, Graham PB, et al. Molecular magnetic resonance imaging of atrial clots in a swine model. Circulation. 2005; 112: 396-9. doi:10.1161/CIRCULATIONAHA.104.529941.

173. Katoh M, Haage P, Wiethoff AJ, Gunther RW, Bucker A, Tacke J, et al. Molecular magnetic resonance imaging of deep vein thrombosis using a fibrin-targeted contrast agent: a feasibility study. Investigative radiology. 2009; 44: 146-50. doi:10.1097/RLI.0b013e318195886d.

174. Spuentrup E, Botnar RM, Wiethoff AJ, Ibrahim T, Kelle S, Katoh M, et al. MR imaging of thrombi using EP-2104R, a fibrin-specific contrast agent: initial results in patients. European radiology. 2008; 18: 1995-2005. doi:10.1007/s00330-008-0965-2.

175. Vymazal J, Spuentrup E, Cardenas-Molina G, Wiethoff AJ, Hartmann MG, Caravan P, et al. Thrombus imaging with fibrin-specific gadolinium-based MR contrast agent EP-2104R: results of a phase II clinical study of feasibility. Investigative radiology. 2009; 44: 697-704. doi:10.1097/RLI.0b013e3181b092a7.

176. Uppal R, Catana C, Ay I, Benner T, Sorensen AG, Caravan P. Bimodal thrombus imaging: simultaneous PET/MR imaging with a fibrin-targeted dual PET/MR probe--feasibility study in rat model. Radiology. 2011; 258: 812-20. doi:10.1148/radiol.10100881.

177. Makowski MR, Forbes SC, Blume U, Warley A, Jansen CH, Schuster A, et al. In vivo assessment of intraplaque and endothelial fibrin in ApoE(-/-) mice by molecular MRI. Atherosclerosis. 2012; 222: 43-9. doi:10.1016/j.atherosclerosis.2012.01.008.

178. Jaffer FA, Tung CH, Wykrzykowska JJ, Ho NH, Houng AK, Reed GL, et al. Molecular imaging of factor XIIIa activity in thrombosis using a novel, near-infrared fluorescent contrast agent that covalently links to thrombi. Circulation. 2004; 110: 170-6. doi:10.1161/01.CIR.0000134484.11052.44.

179. Miserus RJ, Herias MV, Prinzen L, Lobbes MB, Van Suylen RJ, Dirksen A, et al. Molecular MRI of early thrombus formation using a bimodal alpha2-antiplasmin-based contrast agent. JACC Cardiovascular imaging. 2009; 2: 987-96. doi:10.1016/j.jcmg.2009.03.015.

180. Fuster V, Fayad ZA, Moreno PR, Poon M, Corti R, Badimon JJ. Atherothrombosis and high-risk plaque: Part II: approaches by noninvasive computed tomographic/magnetic resonance imaging. Journal of the American College of Cardiology. 2005; 46: 1209-18. doi:10.1016/j.jacc.2005.03.075.

181. Fuster V, Moreno PR, Fayad ZA, Corti R, Badimon JJ. Atherothrombosis and high-risk plaque: part I: evolving concepts. Journal of the American College of Cardiology. 2005; 46: 937-54. doi:10.1016/j.jacc.2005.03.074.

182. van Dam GM, Themelis G, Crane LM, Harlaar NJ, Pleijhuis RG, Kelder W, et al. Intraoperative tumor-specific fluorescence imaging in ovarian cancer by folate receptor-alpha targeting: first in-human results. Nature medicine. 2011; 17: 1315-9. doi:10.1038/nm.2472.

183. Wykrzykowska J, Lehman S, Williams G, Parker JA, Palmer MR, Varkey S, et al. Imaging of inflamed and vulnerable plaque in coronary arteries with 18F-FDG PET/CT in patients with suppression of myocardial uptake using a low-carbohydrate, high-fat preparation. Journal of nuclear medicine. 2009; 50: 563-8. doi:10.2967/jnumed.108.055616.